



The Development of a PocketQube Satellite Communication System

Gary Allen
23905093

Report submitted in partial fulfilment of the requirements of the module Project (E) 448
for the degree Baccalaureus in Engineering in the Department of Electrical and Electronic
Engineering at the University of Stellenbosch.

Supervisor: Dr A. Barnard

November 6, 2023

Acknowledgements

This project would not have been possible without a few acknowledgements. I would sincerely like to thank:

- My supervisor, Dr Barnard, for his input and support throughout the project.
- Mr Peter Roux, for being very helpful and allowing me to test my system on the South African Weather Service balloons.
- My parents, Charleen and Spencer, both for the emotional support that they provided me when stress levels were high, and for the practical support they provided, including driving long distances to test locations far away.
- My friends, for the laughter and support, especially Bevan, who has been a backbone for me while we both worked on our Skripsies together.



UNIVERSITEIT•STELLENBOSCH•UNIVERSITY
jou kennisvennoot • your knowledge partner

Plagiaatverklaring / Plagiarism Declaration

1. Plagiaat is die oorneem en gebruik van die idees, materiaal en ander intellektuele eiendom van ander persone asof dit jou eie werk is.

Plagiarism is the use of ideas, material and other intellectual property of another's work and to present it as my own.

2. Ek erken dat die pleeg van plagiaat 'n strafbare oortreding is aangesien dit 'n vorm van diefstal is.

I agree that plagiarism is a punishable offence because it constitutes theft.

3. Ek verstaan ook dat direkte vertalings plagiaat is.

I also understand that direct translations are plagiarism.

4. Dienooreenkomsdig is alle aanhalings en bydrags vanuit enige bron (ingesluit die internet) volledig verwys (erken). Ek erken dat die woordelikse aanhaal van teks sonder aanhalingsstekens (selfs al word die bron volledig erken) plagiaat is.

Accordingly all quotations and contributions from any source whatsoever (including the internet) have been cited fully. I understand that the reproduction of text without quotation marks (even when the source is cited) is plagiarism

5. Ek verklaar dat die werk in hierdie skryfstuk vervat, behalwe waar anders aangedui, my eie oorspronklike werk is en dat ek dit nie vantevore in die geheel of gedeeltelik ingehandig het vir bepunting in hierdie module/werkstuk of 'n ander module/werkstuk nie.

I declare that the work contained in this assignment, except where otherwise stated, is my original work and that I have not previously (in its entirety or in part) submitted it for grading in this module/assignment or another module/assignment.

23905093 Studentenommer / Student number	Handtekening / Signature
G.V.C. Allen Voorletters en van / Initials and surname	Datum / Date 2023/11/05

Contents

Acknowledgements	A
List of Figures	v
List of Tables	viii
Abstract	x
1. Introduction	1
1.1. Overview	1
1.2. Problem Statement	2
1.3. Requirements	2
1.4. Specifications	3
2. Background	5
2.1. PocketQube	5
2.2. Satellite Tracking	5
2.2.1. Open-Loop	5
2.2.2. GPS (Direct)	6
2.2.3. GPS (Relay)	6
2.2.4. Signal Strength	6
2.3. Antennas	7
2.3.1. Types	7
2.3.2. Feedlines	10
2.3.3. Summary	10
2.4. Telecommunication	11
2.4.1. Modulation Techniques	11
2.4.2. Link Budget	11
2.4.3. Protocols	11
3. System Design	12
3.1. High-Level System	12

3.1.1. Overview	12
3.1.2. Tracking	12
3.1.3. Custom Link	13
3.2. Ground Station	13
3.2.1. Power	13
3.2.2. Communication	14
3.2.3. Steering and Positioning	14
3.2.4. Monitoring	15
3.3. PocketQube Unit	15
4. Detailed Design	16
4.1. Component Selection	16
4.1.1. GPS	16
4.1.2. IMU	16
4.1.3. RF Module	16
4.1.4. Stepper Motor Driver	18
4.1.5. RS-485 Driver	18
4.1.6. Microcontroller	18
4.1.7. Power	18
4.2. Ground Station PCB	19
4.2.1. Circuit Design	19
4.2.2. PCB Layout	20
4.3. PocketQube Unit PCB	20
4.3.1. Circuit Design	20
4.3.2. PCB Layout	21
4.4. Link Budget	21
4.5. Ground Station Antenna	22
4.5.1. Mechanical Considerations	22
4.5.2. Theoretical Design	23
4.5.3. Simulation Design	24
4.5.4. Matching	26
4.6. PocketQube Unit Antenna	27
4.6.1. Mechanical Considerations	27
4.6.2. Simulation Design and Matching	27
4.7. Software	28
4.7.1. Classes	28
4.7.2. Tracking	28

5. Implementation	29
5.1. Ground Station PCB	29
5.2. Ground Station Antenna	29
5.3. PocketQube Unit PCB	30
5.4. PocketQube Unit Antenna	30
5.5. Software	31
5.5.1. Mount Control	31
5.5.2. Pointing	31
5.5.3. Radio and GPS	31
6. Testing	32
6.1. Ground Station PCB	32
6.1.1. Power	32
6.1.2. Motor Drive	32
6.2. PocketQube Unit PCB	33
6.3. Ground Station Antenna	33
6.4. PocketQube Unit Antenna	34
6.5. RF Module	34
6.5.1. Transmit Power Consumption	34
6.5.2. Data Rate	35
6.6. GUI	35
6.7. Range	36
6.8. Tracking and Pointing	37
6.8.1. Open-Loop	37
6.8.2. Closed-Loop	37
6.9. Radiosonde	38
6.10. Full System	38
7. Conclusion	39
7.1. Summary	39
7.2. Future Work	39
Bibliography	41
A. Project Plan	44
B. Outcomes Compliance	45
C. References	47
C.1. PQSU	47
C.2. SUNCQ	48

C.3. Antenna Comparison	50
C.4. Link Configuration Summary	50
C.5. Mount Control	51
D. Design	52
D.1. Power Calculations	52
D.2. Ground Station Schematic	53
D.3. PocketQube Unit Schematic	54
D.4. Ground Station PCB	55
D.5. PCB Errata	57
D.6. Ground Station Antenna	57
D.7. Software	58
D.8. Mount Calibration	59
E. Hardware	60
E.1. Mount Gears	60
E.2. Mount Specifications	61
E.3. Mount Rotation	61
E.4. Existing Mount PCB	62
E.5. PocketQube	63
F. Tests	64
F.1. Open-Loop Pointing Test	64
F.2. Range Tests	66
F.3. GUI	68

List of Figures

1.1. A High-Altitude Balloon Carrying a Nano-Satellite Payload [1]	1
1.2. A CAD Model of a Stellenbosch PocketQube Enclosure [2]	1
1.3. Predicted Balloon Path and Distances	2
2.1. A Stellenbosch PocketQube Backplane PCB [2]	5
2.2. GPS Relay Tracking [3]	5
2.3. Dipole Antenna Geometry	7
2.4. Dipole Antenna Radiation Pattern	7
2.5. A Monopole Whip Antenna in a Plastic Housing	8
2.6. A 21-turn Copper Helical Antenna	8
2.7. Yagi-Uda Antenna Geometry [4]	9
2.8. Two Inverted-F Microstrip Antenna Geometries [5]	9
3.1. High-Level System Diagram	12
3.2. Ground Station System Diagram	14
3.3. PocketQube Unit System Diagram	15
4.1. PocketQube Unit PCB Design (Front)	20
4.2. PocketQube Unit PCB Design (Back)	20
4.3. Simulated Helical Antenna Pattern at $f = 405 \text{ MHz}$ ($f_c = 550 \text{ MHz}$, $G_\lambda = 0.7$)	24
4.4. Simulated Helical Antenna Pattern at $f = 405 \text{ MHz}$ ($f_c = 550 \text{ MHz}$, $G_\lambda = 0.5$)	24
4.5. Simulated Helical Antenna Impedance ($f_c = 550 \text{ MHz}$, $G_\lambda = 0.7$)	25
4.6. Simulated Helical Antenna Impedance ($f_c = 510 \text{ MHz}$, $G_\lambda = 0.6$)	25
4.7. Simulated Helical Antenna Pattern without Cup at $f = 405 \text{ MHz}$ ($G_\lambda = 0.6$, $f_c = 510 \text{ MHz}$)	25
4.8. Simulated Helical Antenna Pattern with Cup at $f = 405 \text{ MHz}$ ($G_\lambda = 0.6$, $f_c = 510 \text{ MHz}$)	25
4.9. Helical Antenna with Matching Strip Model	26
4.10. Simulated Helical Antenna Return Loss vs Frequency	26
4.11. Dipole Model	27
4.12. Simulated 0.45λ Dipole Return Loss vs Frequency	27

4.13. Tracking Algorithm Flow Diagram	28
5.1. Ground Station PCB Implementation	29
5.2. Ground Station Initial Antenna Implementation	29
5.3. Ground Station Mounted on a Tripod	30
5.4. PQ Unit (front) [right] and programmer [left]	30
5.5. PQ Unit Antenna Implementation	31
5.6. Stepper Motor Timing Diagram [6]	31
6.1. Measured Helical Antenna Return Loss vs Frequency	34
6.2. Measured Dipole Antenna Return Loss vs Frequency	34
6.3. TX Output Power vs Current Consumption	35
6.4. LoRa Bit Rate vs Spreading Factor	35
6.5. GUI Monitor after “Calibrate”, “Upload”, and “Set Track Mode”	35
6.6. Measured RSSI vs Distance	36
6.7. Measured SNR vs Distance	36
6.8. GPS Tracking Locations and RSSI Values	37
6.9. Received Radiosonde Signal Spectrum	37
6.10. Radiosonde Closed-Loop Tracking Predicted Path (left) vs Actual (right) .	38
6.11. Radiosonde Closed-Loop Tracking SNR vs Distance	38
C.1. Azimuthal and Elevation Visualization [7]	51
D.1. Ground Station PCB Design (front)	55
D.2. Ground Station PCB Design (back)	56
E.1. The Existing Antenna Mount	60
E.2. Mount Azimuthal Compensation 1 (Elevation Fixed)	61
E.3. Mount Azimuthal Compensation 2 (Elevation Fixed)	61
E.4. Mount Azimuthal Compensation 3 (Elevation Fixed)	61
E.5. Mount Azimuthal Compensation 4 (Elevation Fixed)	61
E.6. Mount Azimuthal Compensation 5 (Azimuth Fixed)	61
E.7. Mount Azimuthal Compensation 6 (Azimuth Fixed)	61
E.8. Existing Antenna Mount PCB (front)	62
E.9. Existing Antenna Mount PCB (back)	62
E.10. PocketQube Breadboard for Testing	63
E.11. PocketQube Unit (back)	63
F.1. Open-Loop Pointing Test Setup	64
F.2. Open-Loop Pointing Test Elevation Angle Measurement	65
F.3. Open-Loop Pointing Test Locations	65
F.4. Range Tests Mapped Locations 1-5	66

F.5. Range Tests Mapped Locations 6-9	66
F.6. GUI Output after Connecting to the Ground Station	68
F.7. GUI Output after Reset, Calibration, and Reset Again	68
F.8. GUI Output while Receiving Telemetry from LoRa Link	69

List of Tables

2.1. Comparison of Modulation Techniques	11
4.1. Comparison of two LoRa modules	17
4.2. Link Budget - Satellite	21
4.3. Link Budget - Channel	21
4.4. Link Budget - Ground Station	21
6.1. Ground Station Voltage Measurements	32
6.2. Motor Drive Operating Tests @ 12 V supply	33
A.1. Initial Project Plan	44
B.1. ECSA Outcomes Compliance 1	45
B.2. ECSA Outcomes Compliance 2	46
C.1. Qualitative Comparison of Antenna Characteristics [8]	50
C.2. Notable SX1278 Configurations [9]	50
D.1. Ground Station Total Power Calculation	52
D.2. PocketQube Unit Component Power Consumption	52
D.3. Helical Antenna Final Parameters	57
D.4. GPS Class	58
D.5. Radio Class	58
D.6. Link Class	58
D.7. StepperMotor Class	58
D.8. Mount Class	58
D.9. GroundStation Class	59
E.1. Mount Gear and Motor Specifications	61
F.1. Range Test Location Descriptions	67

Nomenclature

Acronyms and abbreviations

ACK	Acknowledge
ASK	Amplitude Shift Keying
CAD	Computer-Aided Design
CCSDS	Consultative Committee for Space Data Systems
CRC	Cyclic Redundancy Check
CSP	CubeSat Space Protocol
EIRP	Equivalent isotropic radiated power
EPS	Energy Power System
FSK	Frequency Shift Keying
GFSK	Gaussian Frequency Shift Keying
GNSS	Global Navigation Satellite System
GPS	Global Positioning System
GS	Ground Station
GUI	Graphical User Application
IC	Integrated Circuit
IMU	Inertial Measurement Unit
LEO	Low Earth Orbit
LOS	Line-of-Sight
PCB	Printed Circuit Board
PQ	PocketQube
PQSU	PocketQube Stellenbosch University
PEC	Perfect Electrical Conductor
PSK	Phase Shift Keying
QAM	Quadrature Amplitude Modulation
RF	Radio Frequency
RX	Receive
SF	Spreading Factor
SU	Stellenbosch University
TX	Transmit

Abstract

This report documents the design and implementation of a wireless communication system for a miniaturised satellite called a *PocketQube*. The PocketQube standard is a set of specifications which aim to make it easier for people to design small satellite modules that can easily integrate with each other. The standard is relatively new, however, and few designs have been published for a full PocketQube communication system that includes a ground station.

The design in this project includes both a tracking ground station, as well as a PocketQube module. The LoRa-based ground station was designed to mechanically track the satellite system using a pre-defined GPS path, as well as using satellite-received GPS data. The ground station was also designed to receive telemetry from existing Radiosondes in the meteorological band. The system was then implemented, and the LoRa communication link was successfully tested up to 120 km line-of-sight at a baud rate of 9600 bps. This report documents the design choices made and constraints faced, analyses the measured results of the system, and suggests improvements for future projects.

1. Introduction

1.1 Overview

This project aims to design and implement a wireless communication system for a miniaturised satellite called a *PocketQube* (PQ). The PocketQube standard was created to define physical and electronic requirements for so-called “nano-satellites”, with the goal of easy integration of various sub-modules into one physical enclosure.

Nano-satellites can either be placed into orbit, or attached to a *high-altitude balloon*. One common use-case of these balloons is to collect sensory information from the atmosphere, such as temperature and humidity readings. The goal of this project is to design a system that can be used in a balloon launch from the Saldanha Air Field, which may ultimately be done by the Stellenbosch Engineering department.



Figure 1.1: A High-Altitude Balloon Carrying a Nano-Satellite Payload [1]

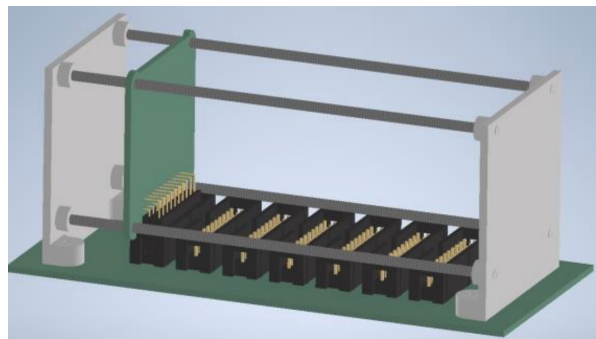


Figure 1.2: A CAD Model of a Stellenbosch PocketQube Enclosure [2]

A satellite communication system includes both a ground station (GS), as well as a module on the satellite itself. The aim of this project is to establish a minimal prototype for both of these systems, so that future projects can refine the developed sub-systems. In this report, general system requirements are first listed, and a problem statement is drawn up. Then, a literature review is conducted to gather background information in the fields of interest. This includes an overview of the PocketQube standard, antenna theory, satellite tracking, and telecommunication theory. A systems level design is then done, which is followed by a more detailed design. Finally, the system is implemented and tested, the results are discussed, and potential improvements and work for future projects are listed.

1.2 Problem Statement

The initial problem statement was simply to design a communication system for a PocketQube, with focus on the ground station. As this is relatively broad, investigation of existing balloon-satellite systems, as well as the launch for this specific PocketQube, was done. An additional requirement that the GS should also be capable of receiving information from commercial *radiosondes* (atmospheric telemetry devices) was also given. The specifications of existing radiosondes is therefore used as a reference, both for the new system's requirements, and as a consideration for system integration.

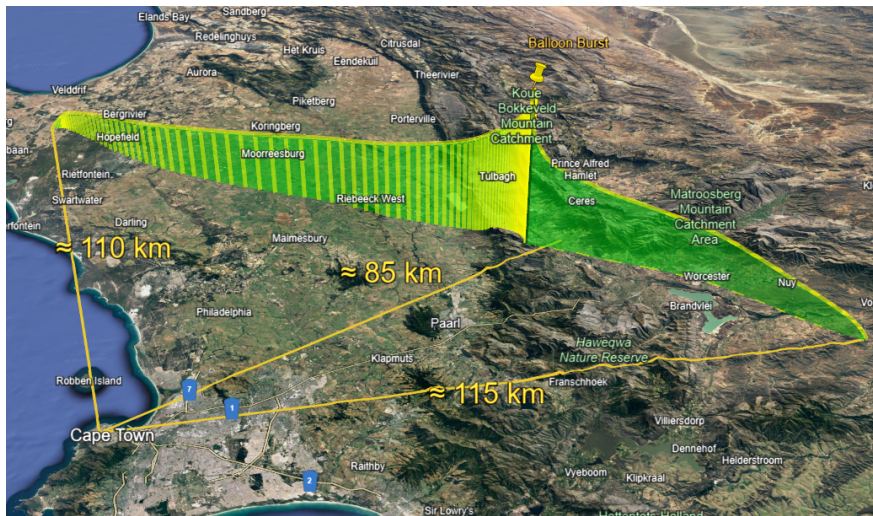


Figure 1.3: Predicted Balloon Path and Distances

High-altitude balloons can drift to a height as much as 30 km above sea level, and can drift as far as 200 km from launch [10]. As mentioned, this project's launch is planned to be near Saldanha Airfield. Using the *HabHub* path predictor [11] on a day where the balloon travels far in-land, a launch from the airfield results in the path as in Figure 1.3. From Cape Town, this is a maximum straight line distance of around 115 km.

A ground station should maintain a reliable wireless link with a satellite to enable continuous communication and real-time telemetry. Since most radiosondes are simply uni-directional "downlink" devices, this should be a priority, however the GS should also be capable of bi-directional communication, in order to issue commands to the satellite.

1.3 Requirements

From the information listed in the problem statement, and after supervisor consultation, slightly more specific user requirements are gathered and listed:

1. The GS should be capable of receiving continuous data wirelessly from the PQ and the Radiosonde. The PQ should be capable of responding to commands from the GS.

2. The communication link should be maintained throughout the predicted path covered in Figure 1.3
3. The PQ unit should remain operational for at least the launch time of the predicted path, which is 2 hours 25 minutes. To cater for longer flights, a goal of 3 hours is set.
4. The PQ unit should conform to the *SU-modified* PQ9 standard (listed in Appendix C.1), and integrate with other prototype units. This standard is here-on referred to as *PQSU*.
5. The GS electronics should integrate into an existing antenna mount, which has been provided by the Department.

The system will undergo a *flight-readiness review* to determine if it has met the requirements before launch. Although the GS could be placed closer to the launch location if the range requirement is not met (while affecting the communication time) this should only be used as a last resort. Further, as the project progresses, if supporting greater distances (> 200 km) will not significantly increase the time, complexity, or cost of the system, it could be catered for as an expansion to the core requirements. It should be noted, however, that the nature of this project (a system prototype) means that such optimisations should not be made a priority.

1.4 Specifications

In order to define a more detailed list of specifications, further calculations should be done. Balloon satellites rise at a vertical speed of around 20 km/h, and safely fall at around 35 km/h after bursting if a parachute is used [10]. The predicted flight path in Figure 1.3 shows a travelled horizontal distance of about 60 km in 40 minutes after the balloon bursts, resulting in a horizontal speed of 90 km/h. A speed of around 100 km/h will be designed for, allowing slightly faster fall speeds.

At a maximum height of 30 km, a calculator reveals that the horizon is around 600 km [12]. The GS antenna could therefore be placed at sea level if communication is only required near maximum altitude. If the balloon should instead be tracked within one minute after launch (300 metres), then a radar horizon calculator reveals that the GS should be placed at an altitude no lower than 200 metres [13], assuming no refraction.

Again referring to the predicted path, a maximum slant range of just over 115 km is obtained, noting that the balloon moves closer as it increases in altitude. For simplification, if the maximum speed (28 m/s) is assumed to occur perpendicular to the ground station at this maximum range, a turn-rate requirement of $t = \frac{v}{r} = \frac{28}{115000} \approx 0.015^\circ/s$ is obtained.

The PQSU standard includes 3.3V and 5V bus voltages. Since this is a prototype launch, there is risk of other units (e.g. the EPS) malfunctioning. A power connection is

also needed for development. A simple battery system which matches the PQSU voltage should therefore be included, to be used both for testing, and potentially for deployment.

Both systems will require PCBs which are constrained in size. PQSU defines the dimensions of a PocketQube PCB i.e. 42 mm x 42 mm outer dimensions, whereas the ground station PCB is constrained to fit onto the provided mount with similar sizing as the previous PCB that was used with it, as shown in Appendix E.4. Lastly, the system should drive the stepper motors which are already provided with the antenna mount, and may make use of the existing zero-sensor. The following system-level specifications are therefore drawn up:

1. The system should be capable of a slant range of 120 km.
2. The GS should be capable of tracking at a turning rate of $0.015^\circ/s$, and the feasibility of various tracking methods (e.g. open vs closed loop) should be explored.
3. The system should be designed to operate at a minimum baud rate of 4800 (which a typical Radiosonde uses [14]) and a target baud rate of 9600 (which is a typical satellite telemetry downlink speed as in [15]).
4. The system should allow for Radiosonde data to be retrieved in the meteorological band between 400.05 and 406 MHz [14]. This data is generally GFSK modulated.
5. A single antenna should be used for both the custom and radiosonde link on the GS, to simplify the design. This antenna should therefore have a bandwidth in the range from 405 MHz up to the amateur radio band (433 MHz).
6. A 100 mW equivalent transmit power restriction should be adhered to.
7. The PQ unit should follow the PQSU and PQ9 standards, which stipulates: a 42 mm square outer PCB dimension; a 4 mm and 2 mm component height above and below respectively; and a 20-pin header interface, catering for RS-485 and I2C communication, and providing 3.3 V and 5 V power lines.
8. The PQ unit should include a battery capable of lasting a minimum of 3 hours at nominal current draw.
9. The GS PCB should integrate onto the existing antenna mount, which has a diameter of 198 mm, with equispaced mounting holes of 3 mm diameter.
10. The GS should be mechanically steered using 4218S-15 bipolar stepper motors, which have a maximum current of 0.50 A per phase, and are driven at 24 V.
11. The GS should provide a USB-C connection to allow a PC to monitor the telemetry data. This should be capable of receiving all data from the link in real-time.

2. Background

2.1 PocketQube

The PocketQube standard is a fairly new set of protocols and specifications defining a modularized nano-satellite system. The term *modularized* in this context refers to the ability for different “modules” or PocketQube units, each with their own set functionality, to be connected to a common *backplane* (as in Figure 2.1) and integrated seamlessly. *Integration* here refers to both the mechanical spacing of each module, as well as the electronic communication between the modules.

As an example, a PocketQube enclosure could contain three units: a communication module, a sensor pack, and a battery system. These modules can then be connected onto a PCB backplane via headers, placed inside a single enclosure, such as that in Figure 1.2, and either launched or released appropriately.

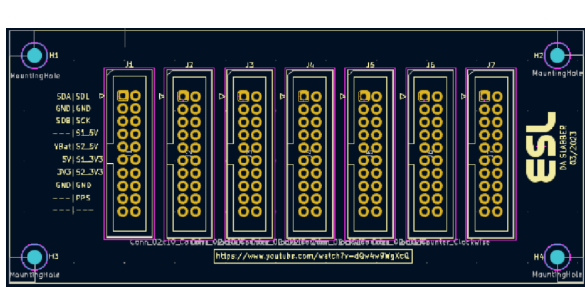


Figure 2.1: A Stellenbosch PocketQube Backplane PCB [2]

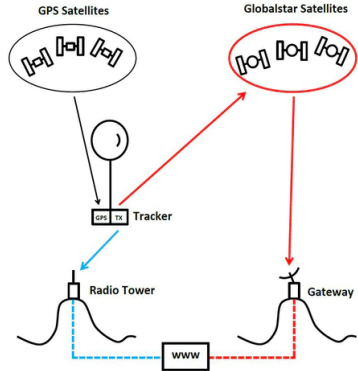


Figure 2.2: GPS Relay Tracking [3]

2.2 Satellite Tracking

2.2.1 Open-Loop

Arguably the simplest tracking method is using what may be referred to as “open-loop” control. Here, only information about the predicted flight path of the balloon/satellite is used, such as expected GPS co-ordinates at different points in time.

Given co-ordinates of both the ground station and the satellite (provided in the *WGS84* system), *Mercator projection* can be used to obtain a cartesian pointing vector [16]. The ground station can then simply be pointed in that direction at each instant in time. The flight path can either be a pre-calculated path (as demonstrated in Figure 1.3), or

can be continuously re-estimated based on real-time weather data. *Habhub* is an online high-altitude path predictor [11] which is freely available.

An advantage of this method is its extreme simplicity to implement. It has several disadvantages, however, including being vulnerable to prediction inaccuracies, as well as the difficulty experienced in re-acquiring the communication link once it is lost. Further, a GPS receiver is generally still required on the ground station, unless it is positioned with a pre-determined location and orientation.

2.2.2 GPS (Direct)

If an initial communication link can be established between the satellite and ground station, *direct* GPS transmission can be added for positional feedback. This is a simple method of “closing” the tracking loop, since the path data can be updated dynamically. Generally, both the PQ and GS GPS co-ordinates are required.

2.2.3 GPS (Relay)

If a link cannot be initially established, a ”relay” method of GPS tracking can be used. This method functions in a three-step process, explained below and depicted in Figure 2.2:

1. The precise position of the payload and the ground station is determined using data received from GPS satellites.
2. The position is *relayed* to an external network (satellite or ground -based) using a radio transmitter.
3. The ground station receives the location from the external network (e.g. via the internet).

The major disadvantage of this method is the additional cost required. Since an antenna capable of communicating with one of the external networks is required, two antennas are needed if direct communication with a ground station is desired (however this is usually no longer necessary as the relay network can be used). Further, the cost of subscribing to an external network is generally high.

This type of tracking works well if the satellite is physically close to the external network satellites, or if the ground station does not need to communicate in real-time, but merely needs access to the location of the satellite e.g. in a home-made balloon satellite launch.

2.2.4 Signal Strength

Radio tracking can be done when the satellite itself transmits omni-directionally. The received signal strength can be used as feedback to determine the direction to point. To

initially find the satellite, the entire sky can be scanned using a "brute force" procedure, or an initial guess can be provided. Then, periodic *radius scanning* can be used to track the signal within a certain portion of the sky, or more advanced techniques such as *conical scanning* can be used, to calculate a new direction to point given a set of conical signal strength measurements.

This method provides great flexibility, since no satellite path information is required, however it is generally not necessary when a reasonable initial guess is available, and an antenna with a reasonably large beamwidth is used.

2.3 Antennas

This section covers a very brief review of different types of antennas in literature, as well as how to practically feed these antennas with a transmission line, and a summary of their varying performances.

2.3.1 Types

There are various antenna types to consider for a satellite communication system. A highly customized design is out of the scope of this project, and therefore only designs with tunable parameters, or existing designs in literature, will be considered. Ultimately, each antenna's *radiation pattern*, *gain* (dBi i.e. decibels relative to an *isotropic* source); fractional *bandwidth*; main lobe *beamwidth*; dimensions; and polarization will be compared. Here, *polarization* refers to the orientation of the EM wave i.e. horizontal, vertical or circular.

Half-Wavelength Dipole

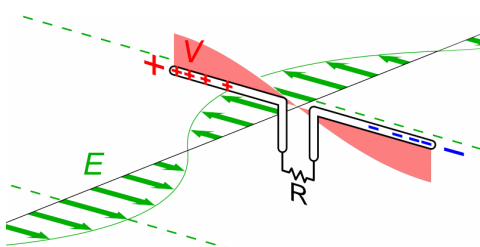


Figure 2.3: Dipole Antenna Geometry

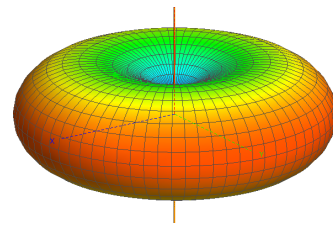


Figure 2.4: Dipole Antenna Radiation Pattern

The half-wavelength (0.5λ) dipole antenna is arguably the simplest and most common type of antenna. It consists of two conductive elements operating in opposite phase, as depicted in Figure 2.3. It is described as having a donut-shaped radiation pattern as in Figure 2.4, with *omni-directional* radiation in the plane perpendicular to the conductor,

and a *null* tangential to the conductor. It has a maximum gain of 2.15 dBi, and is linearly polarized. [8]

Quarter-Wave Monopole

The working principle of a monopole antenna makes use of the electromagnetic theory of *imaging*. If an infinite ground plane or Perfect Electrical Conductor (PEC) is placed below one half of a 0.5λ dipole antenna, since the PEC holds the constraint that the tangential electric field is zero across its boundary, an equal but opposite electromagnetic wave is “induced” due to the incident wave. This wave “appears” to have come from an equal but oppositely polarized “image” source, hence removing the need for the second half of the dipole to be present.

These antennas are extremely useful when size is a constraint, however have the disadvantage of requiring a ground plane. A *whip* antenna is a form of monopole antenna designed to be flexible so that it does not break as easily, and often without a ground plane with reduced performance. It is often placed inside a plastic enclosure, as in Figure 2.5. [8]



Figure 2.5: A Monopole Whip Antenna in a Plastic Housing



Figure 2.6: A 21-turn Copper Helical Antenna

Helical

Helical antennas are coiled windings of wire, where the circumference of the coil has some relationship with the desired frequency. Commonly, a circumference of $C = 1.0\lambda$ is used for *uni-directional* or *axial mode* variants. In this case, a ground plane is required. The ground plane can also be *cuffed* (i.e. extended as an open cylinder) for additional directivity [17]. *Omni-directional* or *normal mode* variants are possible without a ground plane, when $C \ll \lambda$. Figure 2.6 depicts a 21-turn example of such an antenna.

Helical antennas have several design parameters that influence the antenna’s characteristics, such as number of turns (n), wire width (wd), and spacing between turns (S). A spacing of $0.20\lambda < S < 0.25\lambda$ is recommended, however smaller spacings of $0.10\lambda < S < 0.20$ are commonly used [18]. These antennas are also capable of either linear

or circularly polarized signals. Lastly, since they can be designed with an arbitrarily small or large number of turns, and they have a large operating bandwidth, they can be made smaller than other alternatives.

Patch

A *patch* or *PCB* antenna is simply a rectangular PCB trace sized correctly to allow for radiation. Typically, a simple square or rectangular shape can be used. They allow for small profiles at the cost of efficiency [8], and have either circular or linear polarization.

Array

In general, multiple antennas can be combined in an *array* configuration. This allows complete manipulation of the design (such as the desired gain), by virtue of *constructive* and *destructive* interference of the electromagnetic waves. Common variations of this concept reside in *Yagi-Uda* and *Patch Array* antennas. [8]

Yagi-Uda

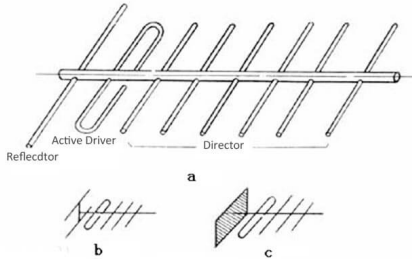


Figure 2.7: Yagi-Uda Antenna Geometry [4]

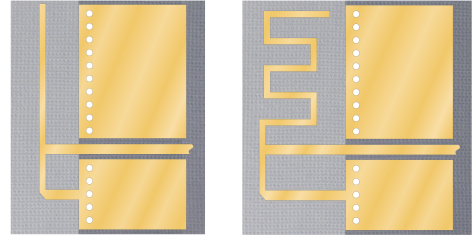


Figure 2.8: Two Inverted-F Microstrip Antenna Geometries [5]

Although not strictly an antenna array, *Yagi-Uda* antennas are one of the most popular directive antennas that make use of interference. A given number of passive conductors are stacked in a specific configuration as shown in Figure 2.7, ultimately steering the EM waves using the concept of interference. Only one of the conductors in the array is fed with the signal. They generally can be made to have very large gain, and are linearly polarized. A *cross-yagi* is a variation on this design which allows for circular polarization.

Microstrip

Microstrip antennas generally refer to any planar, PCB antenna. They can be considered a generalization of a patch antenna. Many variations exist due to their flexible nature. A few examples include: a *patch array*; an *inverted-F* design, which has a small form factor and a nearly 3D omni-directional radiation pattern; a *ring antenna* [19], which is

uni-directional, and has an even smaller form factor than the inverted-F antenna; and a *helical patch* antenna, which is simply a "zig-zag" helix shape flattened onto a PCB.

2.3.2 Feedlines

In general, *feeding* an antenna is more complicated than simply connecting the amplifier's positive and negative terminals to the antenna's terminals. A $50\ \Omega$ characteristic impedance is often used in RF systems. Since each antenna has a unique *input impedance* which is generally different from this value, it must be *matched* appropriately for optimal performance. A few well-known techniques for a number of the antennas in Section 2.3.1 are reviewed below.

General

A general, antenna-agnostic narrow-band technique for antenna impedance matching is to employ a "lumped element" matching circuit consisting mainly of inductors and capacitors. The most common example of this is an L-section, with exactly one capacitor and inductor.

Half-Wavelength Dipole

A half-wavelength dipole antenna has an input impedance of around $73\ \Omega$, varying only due to the wire diameter used. A common method to reduce this impedance to $50\ \Omega$ is simply to reduce the length of the dipole. In this case, a $50\ \Omega$ match occurs from $0.42\ \lambda$ to $0.44\ \lambda$. [17]

Helical

The input impedance of a helical antenna varies between 100 and 200 ohms. A common method to reduce this impedance is for the first quarter turn of the helix to be in the form of a conductive strip, and for the *pitch angle* of this section to be close to zero [17]. The height above the ground plane can then be varied to match the antenna appropriately, with the following equation approximately providing a $50\ \Omega$ match [17]:

$$h = \frac{w}{\frac{377}{\sqrt{\epsilon_r} Z_0}} - 2$$

2.3.3 Summary

It is useful to have a qualitative comparison of different antenna types as a reference for the design phase. This is presented in Table C.1 in the appendix, and has been tabulated using both the previous research, and general consensus in literature. Note that a *narrow* beamwidth generally corresponds to a *uni-directional* antenna (and wide for omni-directional) and therefore this characteristic has not been included in the table.

2.4 Telecommunication

2.4.1 Modulation Techniques

The *modulation* technique used over a digital communication link refers to the method used to represent bits as electrical signals. Common techniques are compared below.

Name	Bit Variation	Comments
Amplitude Shift Keying (ASK)	Amplitudes	Low noise immunity
Frequency Shift Keying (FSK)	Frequencies	<i>Gaussian-FSK</i> (GFSK) is a common variation which filters the signal, decreasing the bandwidth for similar throughput.
Phase Shift Keying (PSK)	Phase Angles	This is often seen as similar to FSK. It is also similar to QAM, but has lower spectral efficiency.
Quadrature Amplitude Modulation (QAM)	Amplitude-Phase Pairs	It has very high spectral efficiency, and is commonly used for higher cost, high throughput systems.
LoRa (“Long-Range”) Modulation	Frequency-varying “Chirps”	It has been seen to drastically increase range, at the expense of greater bandwidth requirements [9]. Its practical use has also been demonstrated in an existing CubeSat system [20].

Table 2.1: Comparison of Modulation Techniques

2.4.2 Link Budget

For any communication system, a *link budget* should be estimated, with the goal of taking into account transmitter power, antenna characteristics, receiver sensitivity, and any attenuation involved. A number of the attenuation affects include: cable loss; amplifier-antenna mismatch; free-space path losses; absorption losses due to clouds and rain; *polarization* mismatch due to antennas not being aligned; *scintillation* effects due to changes in the air’s refractive index; and the effect of varying *elevation angles* [21]. It is recommended to include a minimum *fade margin* of at least 3 dB for low frequency links [22]; 10 dB for links that require more up-time [23]; and 20 dB for critical links.

2.4.3 Protocols

A few link-layer and network-layer protocols already exist that facilitate nano-satellite applications. The CubeSat Space Protocol (CSP) [24] is a fully-fledged network layer protocol for CubeSat embedded systems. It allows for all devices in the satellite ecosystem (satellite modules, the ground station, a control computer etc.) to communicate ”directly” with each other via *packet forwarding*. It relies on various link and network -layer protocols, including KISS, I2C and CCSDS (*Consultative Committee for Space Data Systems*).

3. System Design

3.1 High-Level System

3.1.1 Overview

A complete high-level system block diagram illustrating the system-level decisions is shown in Figure 3.1. This project follows a waterfall methodology, where the functional components of the system are first considered; the systems is designed using a top-down approach; and then the system is tested using a bottom-up approach. Since a large number of sub-systems are required on the ground-station, either IC *modules* or simple *reference designs* will be form the basic building blocks of the system. Only if no modules or designs are found to meet the system requirements, will a more custom solution be developed. The ground station will be powered via +12 V from a battery, and the PocketQube will be powered from an on-board EPS (another PQ unit).

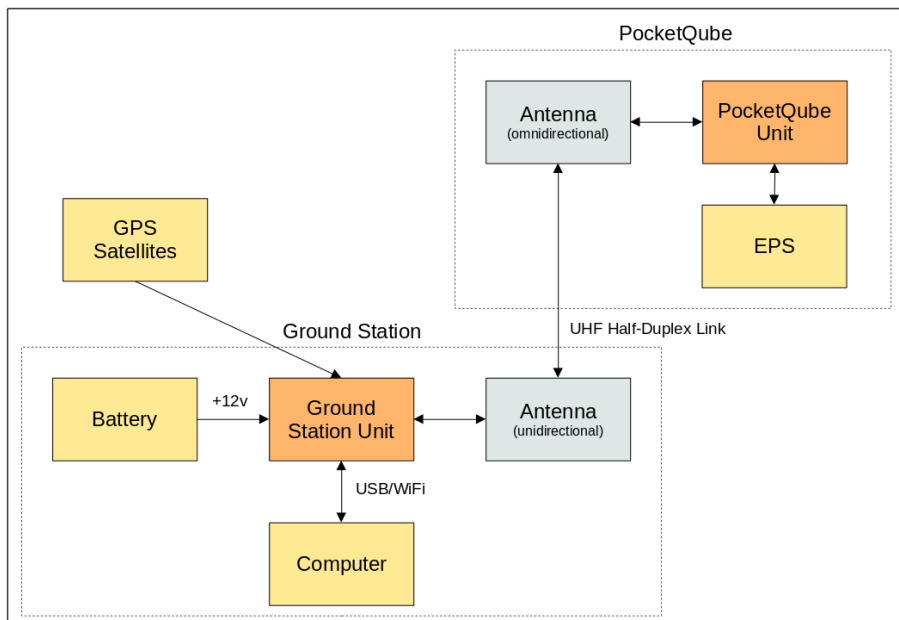


Figure 3.1: High-Level System Diagram

3.1.2 Tracking

Further research shows that trajectory predictions for both the landing area and the dynamic altitude of a balloon can be up to 15-20 km inaccurate for a standard 2 hour flight [25]. For the worst case, this is a total inaccuracy of $\sqrt{20^2 + 20^2} = 28$ km. For the designed range of 120 km, this results in an angle inaccuracy of $360 \times \frac{28}{2\pi \times 120} \approx 14^\circ$.

An antenna with a beamwidth of double this angle is therefore required, to ensure that the satellite is still within the beam even when the antenna's boresight is pointing with worst-case open-loop accuracy. A Yagi-Uda antenna with a beamwidth of around 28° has a gain of around 17 dBi [26]. Using a common Si4311 FSK receiver's sensitivity of -104 dBm, an initial link budget can be estimated. If it is assumed that the link will use 100 mW (20 dB) transmit power, the full 22 dBi gain, and 127 dB path loss attenuation loss at 115 km, then a 10 dB link margin is obtained.

Since the above link budget clearly indicates that open-loop tracking is feasible, it is decided to focus on this as the main tracking method. The ground station therefore requires at least a GPS connection; a means of determining true north (such as a magnetometer); and a means of uploading path data. The path data will be uploaded to the ground station via USB from a system computer. If time allows, direct GPS tracking will then be added as a method of "closing the loop", and to improve pointing accuracy.

3.1.3 Custom Link

A half-duplex link will be designed. This is decided on due to the nature of the link itself (i.e. either downlink "telemetry" or a simple command-response "telecommand" pattern) and due to the added complexity that full-duplex would require (i.e. a dual frequency system).

For the given flight path, a goal of at least 9600 downlink baud rate will be designed for at the 120 km range, with LoRa being explored as the main modulation technique. This is chosen due to the high sensitivity it offers (which will help alleviate the need for a large, high-gain antenna), as well as the link speed it offers for reasonable bandwidth (< 500 kHz). GFSK will be considered as a backup option, since it is well-established in literature. The 433 MHz amateur band (430 to 440 MHz) will be utilized.

3.2 Ground Station

3.2.1 Power

The power section consists of two linear regulators, as well as a boost converter. Since the existing motors are ideally powered from +24V, a boost converter will be used to step up the voltage from a battery voltage of +12V. Further, +5V and +3V3 regulators will be included to power both the MCU and any other ICs. Linear regulators were selected, due to their simplicity, as well as the lack of any specific system-wide efficiency requirements.

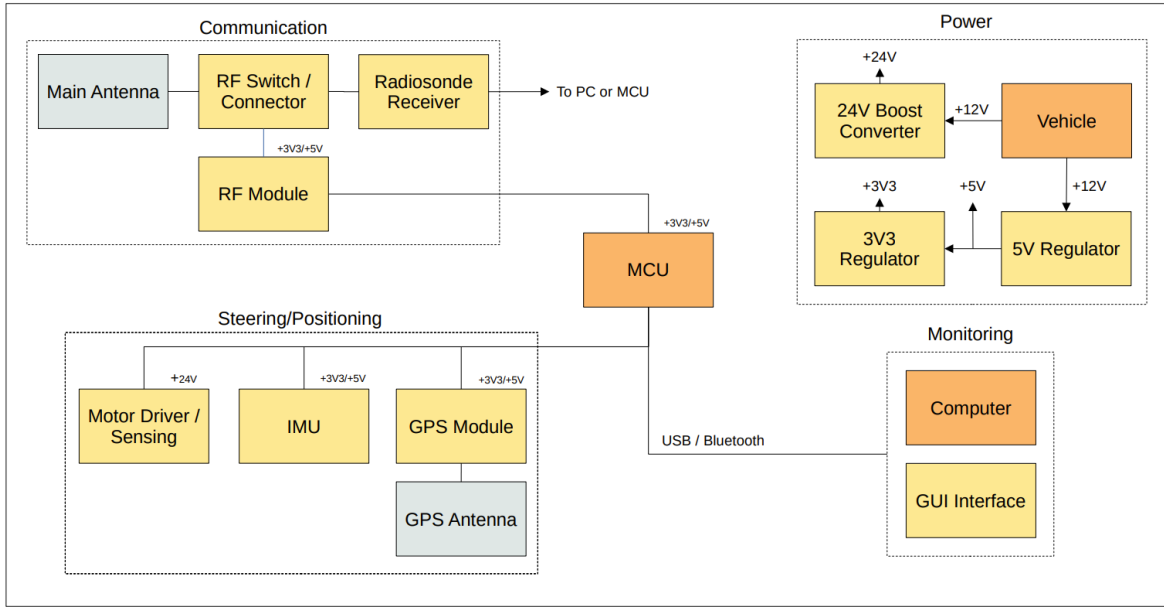


Figure 3.2: Ground Station System Diagram

3.2.2 Communication

The communication section consists of the main antenna, as well as the RF circuitry and connectors. The *RF Switch/Connector* is provided to allow the antenna to be shared between the custom and radiosonde communication links. Initially, a connector will be used for prototyping. If time allows, a dedicated RF switch could be included, which will allow for the MCU to control the antenna connection. The radiosonde will either connect to the PC (e.g. if an SDR dongle is used) or to the MCU (if a dedicated receiver is used).

3.2.3 Steering and Positioning

Generally, the orientation of a ground station's antenna is described by both an azimuthal and an elevation angle (see Figure C.1). The existing two-axis antenna mount which will be used to control these angles is shown in Figure E.1. Since the antenna platform moves relative to the base (where the PCB is mounted), this relative angle needs to be known. Two options to do this are considered:

1. *Open-loop*. The base's absolute orientation is known, and the platform's relative orientation is calculated/looked up based on the stepper motor positions.
2. *Closed-loop*. The platform's absolute orientation is measured in real-time, and this information is fed back into the motor's control system to steer the platform correctly.

Since stepper motors are already included, the *open-loop* method will be considered, however the closed loop method may be implemented if this method is found to lack accuracy, or the motor locations are found to be unpredictable.

3.2.4 Monitoring

A simple Graphical User Application (GUI) will be implemented, allowing the user to control the ground station's orientation (e.g. perform motor calibration); read telemetry received from the satellite; and monitor the link's performance.

3.3 PocketQube Unit

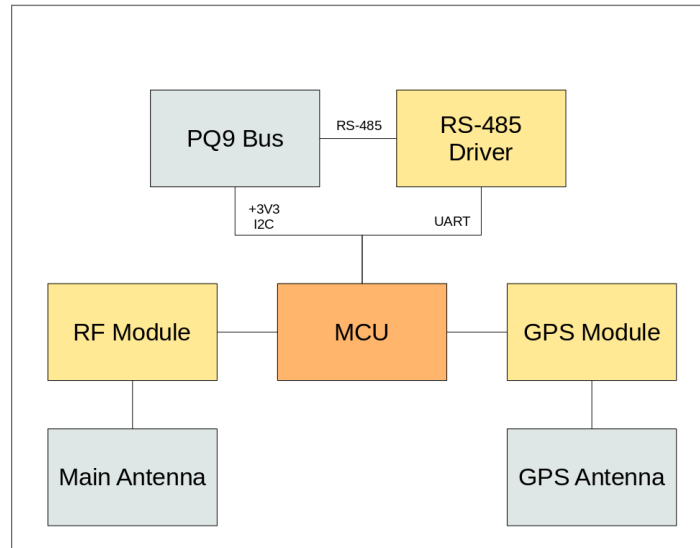


Figure 3.3: PocketQube Unit System Diagram

A block diagram of the system components for the PocketQube unit is shown in Figure 3.3. This unit is relatively simple in comparison to the ground station. The unit consists of an RF section, and a GPS section. The system will be powered via the +3V3 on the PocketQube bus. An integrated GPS module, as well as RF module, should be included. Further, an RS-485 line transceiver should be included to cater for the PQ standard's RS-485 bus, which will likely connect to the MCU via UART.

4. Detailed Design

4.1 Component Selection

Components for the various sub-systems should now be selected. Through-hole components and breakout boards will mostly be used for the ground station, and surface mount components for the PQ unit. Some existing components will be used e.g. the stepper motors, which draw 0.50 A and allow for up to 0.5 N · m of torque [27], and an azimuthal zero-sensing circuit, with a *H22A* optical switch and a low-pass filter.

4.1.1 GPS

The same GPS will be selected for both the ground station and PQ unit to simplify development. A one degree pointing accuracy will be designed for, as it is an order of magnitude less than the beamwidth from Section 3.1.2. A distance of 120 km results in a large required accuracy of $2 \times 120000 \times \pi \times \frac{1}{360} \approx 2 \text{ km}$. The ATGM336H and the *ATGM332D* are two readily-available options that advertise 2.5 m accuracy, which is much better than required. Since both of these also have active antenna support, and current consumption less than 100 mA, the ATGM332D-5N31 is chosen for its lower price.

4.1.2 IMU

To automatically determine absolute ground station orientation, the ground station could include an inertial measurement unit (IMU). Alternatively, a *dead-reckoning* fix can be done by ensuring the ground station is flat and manually positioned to face magnetic north. To provide maximum flexibility in the implementation stage, a 9-axis IMU, which includes both an accelerometer and a magnetometer, will be included. Since the ground station's mount will not be moving, only a low-accuracy accelerometer is assumed to be adequate for orientation. The *MPU-9250* is selected, as it is inexpensive and readily-available.

4.1.3 RF Module

The transciever type for both the custom and radiosonde link needs to be considered. There are a few options in this regard, listed from more to less specialized:

- Fully custom design. Here, components are discretely designed using transistors, DSPs etc. This option is listed for completeness, but is out of scope for this project.

- Front-End Module (FEM). For this option, the FEM provides filters, a low-noise amplifier (LNA), antenna matching, and down-conversion. Then, a controller (e.g. FPGA or MCU) needs to be designed to perform modulation/demodulation functionality (the *modem*) and interface with the FEM.
- Dedicated Transciever. A transciever provides FEM and modulation functionality, however still requires RF techniques for matching, and an additional RF shield.
- Dedicated module. For this option, all functionality is provided in a dedicated module, with a simple antenna connection/pin and an MCU interface. This method has little flexibility, since all matching and design is done internally, and the frequency band is therefore constrained, however provides highest ease-of-use.
- Software-defined radio (SDR). This is the most general-purpose option, but does not exercise the highest performance. It is often directly connected to a computer.

Custom Communication

For the custom link, a dedicated LoRa module will be used. Most of these modules include GFSK as a built-in alternative, making them ideal. All LoRa ICs are based on *Semtech* chipsets due to the company's patent on the technology. Although dedicated transceivers are available, these require special RF considerations to be made, and therefore a module will be utilized to ease development. Table 4.1 contrasts the two most common modules in the 433 MHz LoRa band. The RA-02 is selected due to availability.

Name	RX Sensitivity	TX Sensitivity	Frequency
RA-02	-141 dBm	+18 dBm	410 to 525 MHz
RFM98	-148 dBm	+20 dBm	410 to 525 MHz

Table 4.1: Comparison of two LoRa modules

Radiosonde Communication

Unfortunately, although the selected LoRa module supports GFSK demodulation, it does not receive in the meteorological band, and therefore a second receiver is needed for the radiosonde link. To cater for a wide variety of radiosondes, a software-defined radio (SDR) will be used to adjust the decoding parameters dynamically. The *RTL-SDR* USB dongle is considered the standard, low-cost solution for this, and is therefore selected. An alternative option is to design a dedicated GFSK receiver which allows for adjustable parameters, however this route is not chosen due to time constraints.

4.1.4 Stepper Motor Driver

The original PCB of the previous antenna mount contained two A3972 ICs to drive the stepper motors. Although these could be de-soldered and used, it is favourable to use a newer IC for replacement in case of damage. From the driver and motor datasheets, it is realized that the drivers should operate in dual DMOS full-bridge output configuration; allow bipolar PWM current control; allow for micro-stepping; and provide 0.5 A at 24 V. Very few drivers fit these exact specifications. The *A4970* is considered the follow-up version of the *A3972*, however is not available in a single pack or locally. The *L6219* driver is found to match most specifications, while only allowing half-stepping. It is therefore selected, as there is no noise requirement for the system, and a single step is calculated at 0.22° and 0.45° for the elevation and azimuthal axes, which is small.

4.1.5 RS-485 Driver

An RS-485 driver is needed for compatibility with the PQ bus interface. Due to the project's nature (i.e. all units on the bus are physically close units) only short-range RS-485 communication should be catered for. Further, the PQSU standard specifies no speed requirements, and therefore a minimum of 9600 baud will be designed for. The *MAX485* is selected both due to its availability, and the fact that it meets these specifications.

4.1.6 Microcontroller

An MCU will be needed both on the GS and the PQ. The ESP32, Arduino, and STM32 frameworks are considered. The *ESP32-WROOM-32* is a commonly available ESP32 variant which has 32 GPIO pins. It is also has several ADCs, and allows for both WiFi and Bluetooth connectivity. The *ATMEGA328PB* is an MCU commonly used in small Arduino boards. It has fewer pins than the ESP, is an 8-bit MCU, and has only 32 KB of flash memory, but allows a supply voltage of as low as 1.8 V, and has very low current consumption. Finally, the common *STM32F411* MCU is a high-performance Arm-based MCU, advertised to have highly accurate ADCs and up to 81 GPIOs. Since the processing requirements for this project are assumed to not be high, and the ESP32 is a relatively high-performance MCU which satisfies the pin requirements it will be selected for the GS. For the PQ unit, the ATMEGA328PB will be used, due to its exceptionally low current consumption, and many fewer pins being needed for the PQ unit.

4.1.7 Power

Both the ground station and the PocketQube should cater for the three-hour flight time. Component power calculations are listed in Tables D.1 and D.2, resulting in 50 W and 453 mW for the GS and PQ respectively. A 12 V lead-acid battery will be used for the

ground station. This should be capable of supplying around 4 A, resulting in a capacity requirement of 12 Ah. A more readily available 7.2 Ah battery will initially be used for development. Linear regulators will be used for the 3.3 V and 5 V supply (as opposed to switched-mode) due to their simplicity and the lack of any system-wide efficiency specifications. The 3.3 V regulator should be capable of supplying around 130 mA to the RF module, GPS, and IMU, and the 5 V regulator around $120\text{ mA} + 130\text{ mA} = 250\text{ mA}$ for the other components. The LD1117CV and L7805CP are readily-available linear regulators which can supply up to 800 mA and 1.5 A respectively, and therefore meet these requirements. A boost converter will be used to achieve the 24 V motor drive voltage, which should support 2 A at its 12 V input due to the motors drawing 0.5 A per coil. A breakout board based on the XL6009 IC will be used, which meets this requirement. For the PocketQube unit, the LiPo battery should be capable of supplying around 120 mA nominally. To achieve the 3 hour specification, a capacity of 360 mAh is required. A larger 2000 mAh battery will be used for development, due to its low-cost; the added convenience of fewer discharge cycles; as well as the allowance it provides for retrieving the payload after the balloon has landed at the end of the day (≈ 16 hours later).

4.2 Ground Station PCB

4.2.1 Circuit Design

For the ground station schematic, “typical application” circuits found in component datasheets were mostly used. The final schematic can be found in Appendix D.2.

Motor Drivers

The L6219 drivers require a reference voltage to set the maximum current. According to the datasheet [6], a peak current of $I_{max} = 10 \times \frac{V_{ref}}{R_s}$ in mA is used. Since the recommended value of $R_s = 1\Omega$ is being used, $I_{max} = 10 \times V_{ref}$ mA. Since the motors allow up to 500 mA per winding, a current value of $I_{max} = 475$ mA is chosen to prevent damaging the motors. Therefore, $V_{ref} = 4.75$ V. This can be implemented with a voltage divider. Setting the upper resistor $R_1 = 1\text{k}\Omega$ results in $R_2 \approx 20\text{k}\Omega$, as shown in the schematic. The disadvantage of this method is that the maximum current cannot be controlled dynamically. The reference can be replaced with a DAC from the MCU if more control is required.

Connectors

The RA-02 RF module states that not all data pins are necessary. Further, it was assumed that there may be some errors in the original design. A male header was therefore provided for unused GPIO pins, to allow for flexibility once the PCB was manufactured.

4.2.2 PCB Layout

A 2-layer stackup was decided on, since the in-house PCB machine has a 2-layer limitation, and it is desireable to manufacture the board as early as possible. The final PCB was designed in KiCAD. The layout is shown in Appendix D.4. Female headers were used for most of the modules, since development boards were being used. Two PCB pours were exposed below the voltage regulators to act as a heat sink for added dissipation.

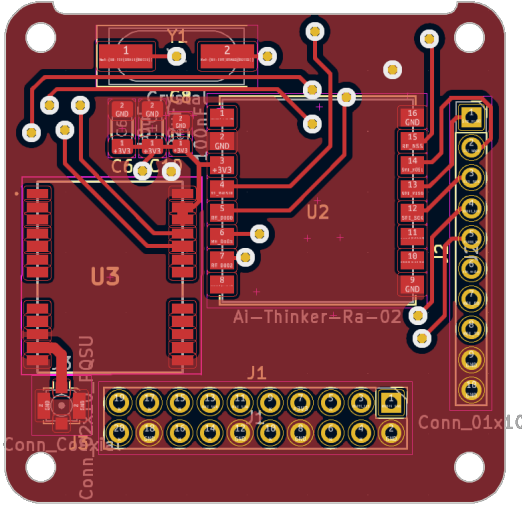


Figure 4.1: PocketQube Unit PCB Design (Front)

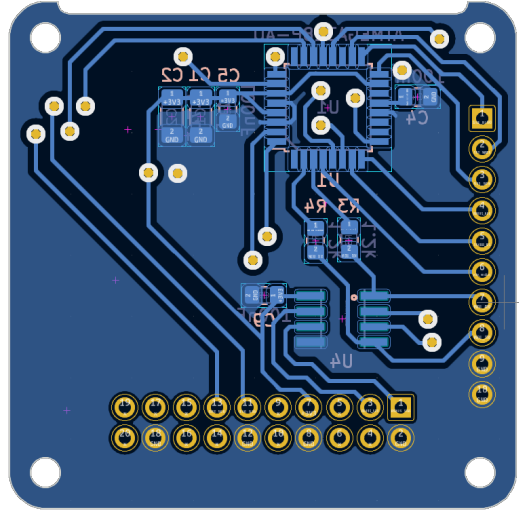


Figure 4.2: PocketQube Unit PCB Design (Back)

4.3 PocketQube Unit PCB

4.3.1 Circuit Design

For the circuit design, the Arduino Nano schematic [28] was consulted as a reference. The pins needed to flash the MCU were exposed directly, instead of integrating a USB connection, for simplicity. The final schematic can be found in Appendix D.3.

RF and GPS Modules

Since the RA-02 RF module has a u.FL connector onboard, no considerations need to be taken with respect to impedance matching. The ATGM332D GPS module, however, directly exposes its RF input via one of its SMD pins. The higher L1 GPS band operates around 1575.42 MHz, which is a wavelength of $\frac{3e8}{1575.42e6} = 190$ mm. The “critical length” (the length at which reflections can be ignored) is therefore around 19 mm. If the module-antenna trace length is kept shorter than this, impedance matching will not be necessary.

4.3.2 PCB Layout

It was decided to use a 2-layer board, due to the low component count. Although the impedance matching is not necessary for the GPS module, it is still desirable to control the trace impedance as much as possible. However, a 50-ohm trace on a 2-layer board is around 2.8 mm (determined using a microstrip impedance calculator). This is much larger than the GPS module pad sizes. The trace was therefore made as wide and as short as possible. The final PocketQube PCB is shown in Figures 4.1 and 4.2.

4.4 Link Budget

The link budget should now be estimated, and initial considerations for the ground station's base location should be made. Signal Hill in Cape Town is a viable location, and is easily accessible. At its distance of 114 km, however, one would need to be at a height of 950 m for communication from launch (due to the earth's curvature). Since the balloon would become visible at an altitude of 600 m (from Signal Hill's 350 m height) this location is chosen, since this is only 12 seconds after launch (if an ascent rate of 5 m s^{-1} is assumed). A maximum elevation angle of 16.72° at 30 km altitude should therefore be considered. Notable configurations for the SX1278's sensitivity (the minimum receivable power level) are listed in Table C.2.

Transmitter Power	18 dBm
Mismatch Loss	(0.5 dB)
Transmission Line Loss	(1 dB)
Antenna Gain	2.15 dB
EIRP	18.65 dBm

Table 4.2: Link Budget - Satellite

Free space path loss (114 km)	126.3 dB
Atmospheric loss	0.22 dB
Scintillation loss	0.37 dB
Polarization Mismatch	3 dB
Total Loss	129.89 dB

Table 4.3: Link Budget - Channel

Antenna Gain	2.15 dBi
Mismatch Loss	(0.5 dB)
Transmission Line Loss	(1 dB)
Receiver Sensitivity	119 dBm
GS Sensitivity	119.65 dBm

Table 4.4: Link Budget - Ground Station

The LoRa “target bit rate” sensitivity value of -119 dBm ($\text{SF} = 8$ and $\text{BW} = 500 \text{ kHz}$) is decided on, since it provides the 9600 baud rate with some margin. An online path loss calculator at [29] was used to calculate attenuation due to distance, and the Python tool *link budget* was used to calculate atmospheric losses. All values were based on both the

RA-02 and the SX1278 chip specifications; dipoles as antennas; an impedance mismatch loss of 0.5 dB (around -10 dB return loss); and a maximum transmitter power setting (18 dBm). The final link budget therefore results in $18.65 \text{ dBm} - 129.89 \text{ dB} + 119.65 \text{ dBm} = 8.41 \text{ dB}$ of link margin. Although this is theoretically adequate (above the 3 dB recommendation), there are some additional considerations. Firstly, if a higher bit rate is required, e.g. 38.4 kbps, then the margin drops to -2.6 dB. Secondly, if a longer range is required (e.g. for future projects), free space path loss will drastically increase. For example, for a 250 km range, the loss becomes 133 dB, meaning the margin drops to only 1.1 dB. The system will therefore be designed for a 10 dB link margin. An antenna with at least 2.59 dBi additional gain (i.e. 4.74 dBi gain total) should therefore be designed for the ground station. Then, if necessary, the 20 dB recommendation can be reached by lowering the LoRa spreading factor (SF) to support any "mission critical" requirements.

4.5 Ground Station Antenna

4.5.1 Mechanical Considerations

The existing antenna mount is shown in Figure E.1. Azimuthal and elevation stepper motors are connected directly through Gear A and B respectively. Gear A rotates the centre shaft to provide azimuthal steering, whereas Gear B rotates through Gear D and E to allow a change in elevation. The specifications in Table E.1 were realized.

The black plastic platform is triangular and has three mounting holes. The new ground station's antenna should therefore be mounted onto this platform. It is important to consider the forces/torques involved, as well as the stepper motor holding torques, in order to determine the maximum weight and acceptable form factor of the new antenna.

The azimuthal motor need not be considered, as all torques from the mount to its base are perpendicular to the central shaft, meaning it would only need to overcome static frictional forces to rotate the antenna, which are assumed to be negligible. The holding torque of the elevation motor, however, will constrain the antenna design. The holding torque of each motor is 0.25 Nm. The gearing ratio resulting from Gears B, D and E, results in an around 8x torque increase. This provides a holding torque of around 2 Nm at the pivot axle.

The centre of gravity of the antenna, as well as its weight, will affect the motor's ability to hold it in place. The horizontal distance between the pivot axle and the mount in the upright position is measured to be 40mm. Therefore, in the worst-case (when the mount is upright as in Figure E.1) a planar antenna could weigh up to $\frac{2}{(9.8 \times 0.04)} = 5.1 \text{ kg}$. In general, the "mass-distance" product of the antenna (mass times distance of centre of gravity from mount) should not be more than 0.2 kg · m. This should be strongly considered if a longer antenna is desired.

The physical dimensions of the antenna's ground plane is also constrained. A circular ground plane may make contact with the mount's base at low elevation angles (assuming the ground station itself is raised above the ground). When the mount is resting, this constraint is imposed when the ground plane first makes contact with the mount's base. For a circular ground plane, this is around 360 mm diameter at an elevation angle of around 35 degrees.

4.5.2 Theoretical Design

As discussed, the antenna should be capable of receiving from both radiosondes (around 405 MHz), as well as the custom LoRa-based link in the amateur radio band of 430 to 440 MHz. A helical antenna is suggested, for the following reasons:

- Ability to increase gain arbitrarily by increasing the number of windings
- High fractional bandwidth of 50% to 60%, which may allow for a smaller antenna
- Ease of manufacture

The centre frequency f_c of the antenna should first be selected. With a fractional bandwidth of 56%, the inequality $f_c \times (1 - \frac{0.56}{2}) < 405$ MHz must hold. This gives an upper bound on the centre frequency of 562.5 MHz. A minimum ground plane diameter of no smaller than 0.5λ is recommended in [17], and 0.75λ in [30]. It is, however, probable that a ground plane as small as 0.5λ will adversely affect the radiation pattern near the end of the specified bandwidth.

Assuming the larger ground plane recommendation, the resulting ground plane diameter is $0.75 \times \frac{3e8}{562.5e6} = 400$ mm, which is larger than the mechanical size constraint. Nevertheless, $f_c = 550$ MHz is chosen as the initial centre frequency for simulations. the ground plane will then be decreased in size appropriately (towards $G_\lambda = 0.5$ i.e. 270 mm) and the results observed.

The design parameters for a helical antenna are f_c (centre frequency), n (number of turns), S (the spacing between turns), C (the circumference) and G (the ground plane diameter). Design formulae are provided in [17], and have been modified below to use relative values instead of absolute ones (i.e. S_λ and C_λ instead of S and C). Directivity, in dBi, is given by:

$$D_0 = 10 \log(15 \cdot nS_\lambda \cdot C_\lambda)$$

C_λ is typically kept at 1.0, meaning the circumference is equal to the operating wavelength. As mentioned, a gain of around 5 dBi is required. However, a 3 dB bandwidth drop is estimated nearer to 400 MHz since it as the edge of the operating band. Further, the effect of a smaller ground plane will likely decrease performance by an estimated minimum of at least 1 dB. Therefore, a centre-frequency gain greater than 8 dBi will be designed for.

This will also move the system towards the 20 dBi link margin. For this gain, the nS_λ product should equal around 0.45. Although the optimal value for S_λ is 0.23 [17], smaller values have been quoted to work [18] and are mechanically easier to construct. Therefore, $S_\lambda = 0.15$ is chosen, and finally, $n \geq 3$.

4.5.3 Simulation Design

Simulation of a helical antenna is well documented in literature, and therefore the parameters can be varied iteratively and integrated into the antenna design process. For this project, FEKO software is used.

An initial model with the above parameters and a wire diameter of 2.5 mm (chosen due to availability) is simulated at the lower frequency of $f = 405$ MHz. This is done for ground plane sizes $G_\lambda = 0.5$ and $G_\lambda = 0.7$ ($G = 273$ mm and $G = 382$ mm). Most of the follow-up design is conducted around this frequency.

The resultant radiation patterns are shown in Figures 4.3 and 4.4 respectively. It is clear that the recommended value of $G_\lambda = 0.5$ from [17] will not work near this lower frequency, as shown by the morphed radiation pattern. The pattern is found to be acceptable at around $G_\lambda = 0.7$.

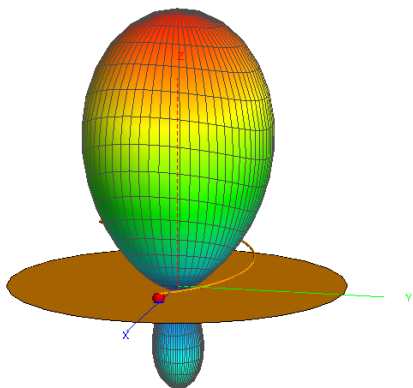


Figure 4.3: Simulated Helical Antenna Pattern at $f = 405$ MHz ($f_c = 550$ MHz, $G_\lambda = 0.7$)

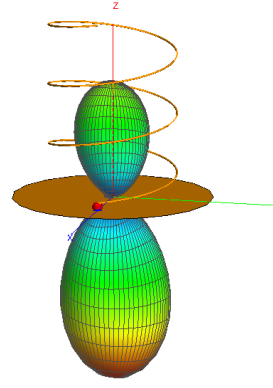


Figure 4.4: Simulated Helical Antenna Pattern at $f = 405$ MHz ($f_c = 550$ MHz, $G_\lambda = 0.5$)

However, after analysing the input impedance for $G_\lambda = 0.7$ with this centre frequency (shown in Figure 4.5) it is clear that broadband matching would be difficult, due to the drastic change in impedance near the lower end of the spectrum. In order to ease matching, a lower centre frequency should ideally be used, to move the input impedance at 405 MHz and at 433 MHz closer together. This will, however, require either a larger ground plane, or a cupped ground plane (discussed further on). Unfortunately, FEKO does not allow for an optimisation goal that depends on two frequencies. Therefore, an iterative approach was used to find the centre frequency which minimizes the difference between the two

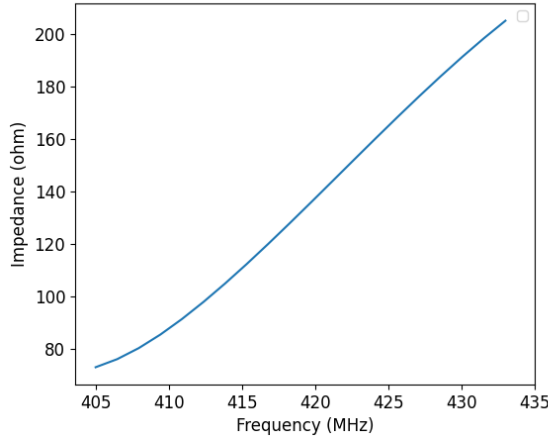


Figure 4.5: Simulated Helical Antenna Impedance ($f_c = 550$ MHz, $G_\lambda = 0.7$)

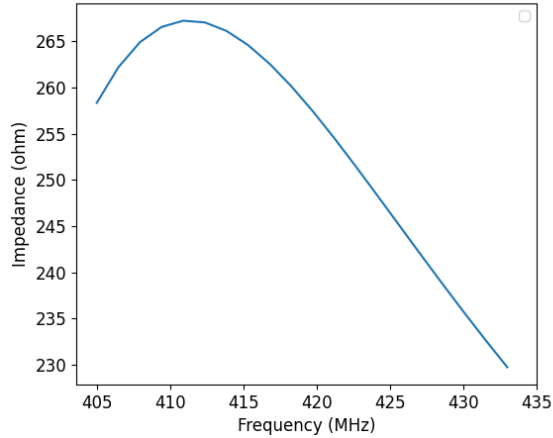


Figure 4.6: Simulated Helical Antenna Impedance ($f_c = 510$ MHz, $G_\lambda = 0.6$)

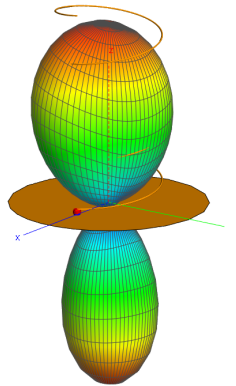


Figure 4.7: Simulated Helical Antenna Pattern without Cup at $f = 405$ MHz ($G_\lambda = 0.6$, $f_c = 510$ MHz)

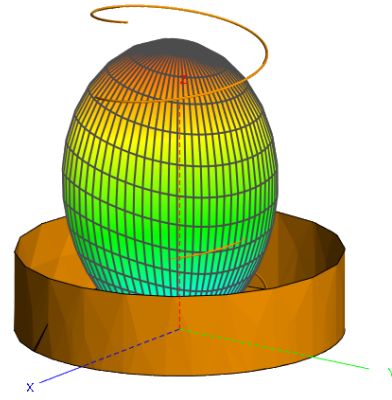


Figure 4.8: Simulated Helical Antenna Pattern with Cup at $f = 405$ MHz ($G_\lambda = 0.6$, $f_c = 510$ MHz)

impedances. The resulting centre frequency was found to be around $f_c = 510$ MHz at $G_\lambda = 0.6$ (≈ 350 mm), with a resultant impedance close to 250Ω (as shown in Figure 4.6).

Since the mount can support a larger weight than the 3 turn coil, it was decided to experiment with larger a turn count (i.e. $n = 4$), both for increased directivity/performance, and to potentially cater for manufacturing imperfections, such as a thin aluminium foil ground plane, and any diversions from the ideal helical shape. It was found that, for small ground plane diameters, as the number of turns increased, the radiation pattern for $f = 405$ MHz was negatively affected. This is intuitive when referring to image theory, as the non-idealities due to the finitely-sized ground plane become more apparent as distance to the plane increases. It should be noted that the pattern at $f = 433$ MHz was not as adversely affected.

The ground plane was therefore cupped, and the results observed. At $G_\lambda = 0.6$, a cup height equal to 1 helical turn was found to greatly improve the radiation pattern. This is

shown in Figures 4.7 and 4.8. The gain, however, was not as drastically affected.

It was therefore decided that the antenna would initially be built with a large ground plane and higher number of turns. Then, after measurement results and protocol implementation, the ground plane would be decreased appropriately to fit onto the mount. If time allows, and it is deemed necessary, a cup will then be added to the ground plane, to improve the pattern and antenna performance, and cater for the radiosonde link. The final model parameters are then $D = 187.1$ mm, $S = 88.2$ mm, $n = 4$, and $G = 350$ mm.

4.5.4 Matching

Impedance matching should be done if the helical antenna is to be fed by a 50Ω coaxial cable. It was decided to match the antenna to the custom link's frequency of $f = 433$ MHz using the strip method mentioned in Section 2.3.2 for an uncapped ground plane. The FEKO model for this method is shown in Figure 4.9.

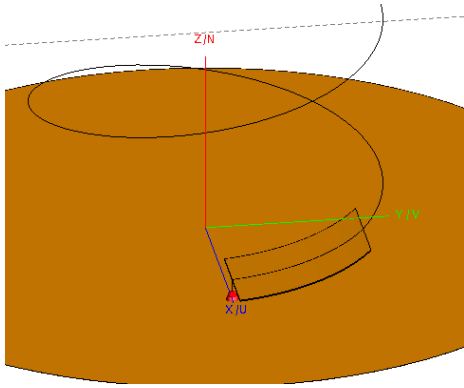


Figure 4.9: Helical Antenna with Matching Strip Model

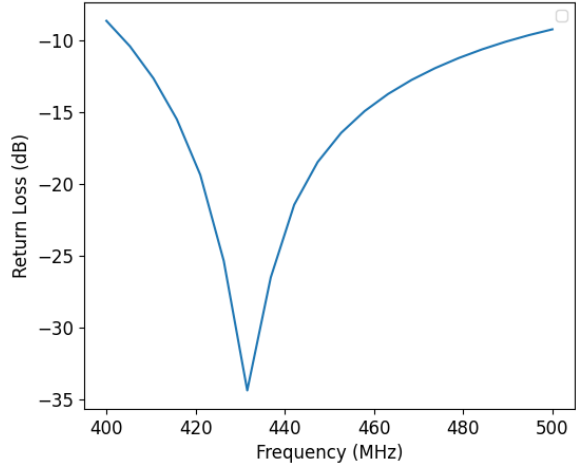


Figure 4.10: Simulated Helical Antenna Return Loss vs Frequency

The strip is recommended to be relatively flat, and extend for approximately the first quarter turn. Its pitch angle was therefore chosen to be half that of the full helix, and it was chosen to extend for 0.15 turns. The unknown parameters for the strip are then its height above the ground plane (also the height of the coaxial pin), and its strip width. The FEKO optimiser was used to optimise these two parameters for a minimum return loss. The resulting return loss as a function of frequency is shown in Figure 4.10. The resultant mismatch loss is close to 0 dB at the target frequency, and 0.451 dB at 405 MHz. The final antenna parameters can be found in Table D.3 in the Appendix. The simulated antenna gain was 7.5 dBi, resulting in a final designed link margin of 12.8 dB. The final simulated beamwidth was 75 degrees.

4.6 PocketQube Unit Antenna

4.6.1 Mechanical Considerations

Since the system is constrained close to the 433 MHz band (due to the radiosonde link), the wavelength of interest is relatively large (693 mm), and one half of a half-wavelength dipole is around 173 mm. Special consideration would be needed to fit this onto the planned PocketQube length of 150 mm. For the planned prototype balloon satellite launch, it is therefore decided to design a half-wavelength dipole, and allow it to simply protrude out the ends of the PocketQube housing from launch. Recommendations for future projects are given in Section 7.2, such as designing a deployable antenna.

4.6.2 Simulation Design and Matching

A simple 1.5 mm metal wire will be used for the dipole due to its availability, and will be fed by a coaxial cable. The design parameters for the dipole are L_λ (the total dipole length relative to lambda), F_{gap} (the gap distance of the feed), and F_{length} , the length of the feed. A fixed gap distance of $F_{\text{gap}} = 5 \text{ mm}$ is decided on, as it is assumed to not be critical if sufficiently small.

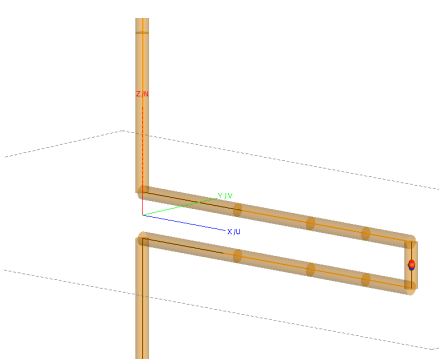


Figure 4.11: Dipole Model

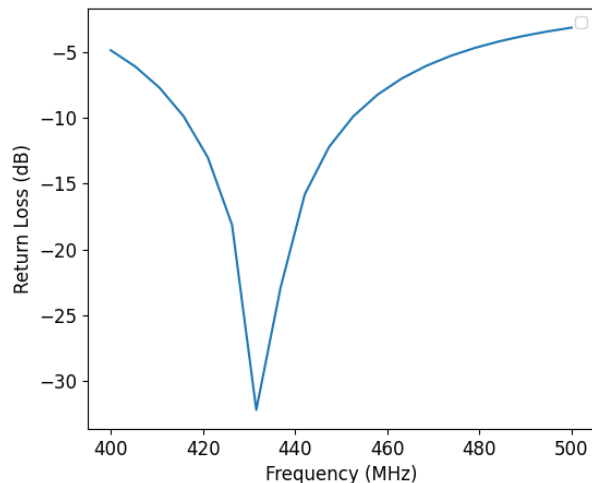


Figure 4.12: Simulated 0.45λ Dipole Return Loss vs Frequency

The FEKO model in Figure 4.11 was used. The optimiser was used to calculate the optimal dipole length and feed length that would minimize the return loss for $f = 433 \text{ MHz}$ at a feed impedance of 50Ω . The resultant parameters are found to be $L_\lambda = 0.45$ ($L = 312 \text{ mm}$) and $F_{\text{length}} = 39.0 \text{ mm}$. The optimised return loss as a function of frequency is shown in Figure 4.12. The radiation pattern was found to be the classic “donut” shape, with a maximum directivity of 2.1 dBi.

4.7 Software

4.7.1 Classes

The Arduino framework will be used, as well as a custom C++ library for re-usability across GS and PQ code. Tables D.4 to D.9 in the Appendix describe expected class functionality. Although the CSP protocol was considered, it was decided to rather develop a simple ASCII protocol between the PQ and GS, encapsulated in the *link* class. The link class was initially cater for downlink telemetry, but can easily be expanded on should satellite commands be required. The *PqTnc* (PocketQube Terminal Node Controller) and *PqUnit* classes were designed as Singleton classes for the GS and PQ respectively. A serial protocol titled *SUNCQ* was drawn up for the PqTnc-to-host communication and can be found in Appendix C.2.

4.7.2 Tracking

For path tracking, it is decided to store data in the TNC object on the ESP32 itself, instead of streaming it from the host computer. This is so that the host can be disconnected, and the payload will still be tracked. The tracking algorithm which caters both for open-loop and closed-loop methods is depicted in Figure 4.13.

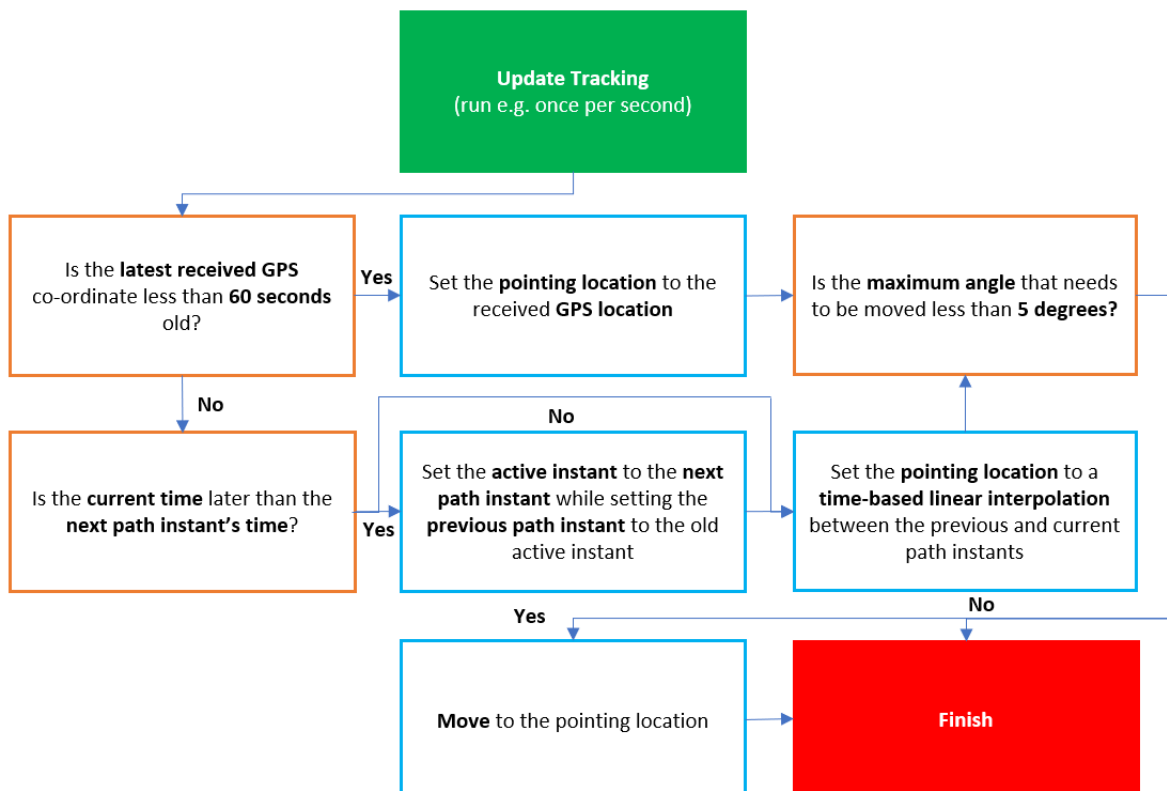


Figure 4.13: Tracking Algorithm Flow Diagram

5. Implementation

5.1 Ground Station PCB

The ground station PCB was manufactured in-house. A figure of the PCB with components assembled, as well as a helical antenna attached for initial development, and a monopole GPS antenna, is shown in Figure 5.1. Some additional wired connections were made to due layout errors. A list of errata can be found in Appendix D.5.

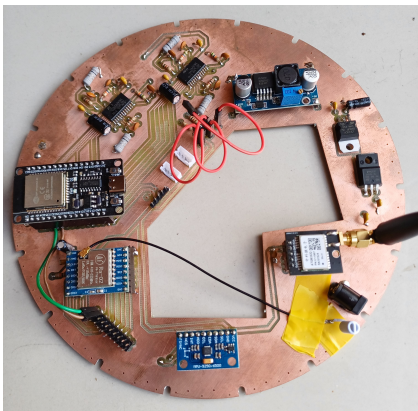


Figure 5.1: Ground Station PCB Implementation

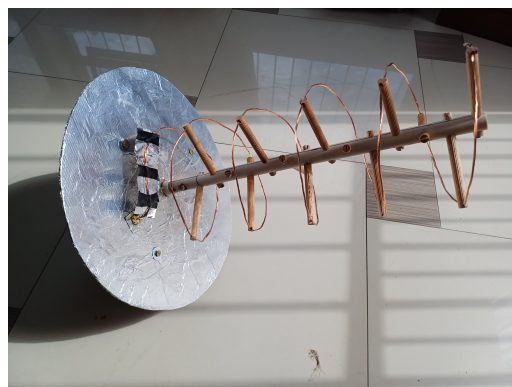


Figure 5.2: Ground Station Initial Antenna Implementation

5.2 Ground Station Antenna

The initial helical antenna build is shown in Figure 5.2. 2.5 mm stranded copper wire was used due to its flexibility and availability. A cardboard ground plane wrapped in aluminium foil was used due to its lightweight nature. Further, a strip of harder aluminium tin was taped to the wire for the matching strip. Initially, the strip was over-sized, and more turns than necessary were used. A female panel-mounted SMA connector was mounted using bolts, and the antenna wire was soldered to the protruding pin. The coiled wire is mechanically supported by a central PVC pipe and wooden dowels. Markings on the pipe were used to dimension the antenna. The materials were sized to provide stability, but not exceed the maximum torque limitations of the motors. The final antenna weight was measured at 344 g, giving a worst-case mass-distance product of $344 \text{ g} \times \frac{45 \text{ cm}}{2} \approx 0.08 \text{ kg} \cdot \text{m}$, which is under the maximum of 0.2 kg · m. After initial testing, the matching strip was cut to size, a circular trapezoidal cut-out was made to support a lower elevation angle, and the number of turns was set to $n = 4$. The system was eventually mounted onto a tripod, and a final photo of the full ground station out in the field is shown in Figure 5.3.



Figure 5.3: Ground Station Mounted on a Tripod

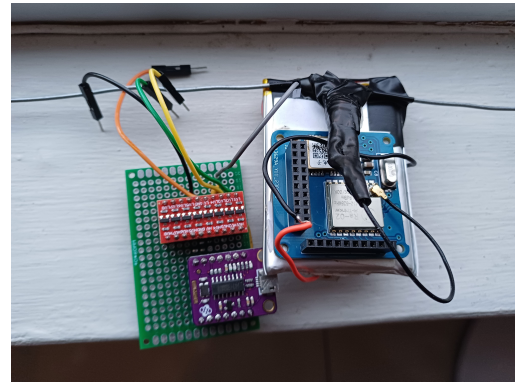


Figure 5.4: PQ Unit (front) [right] and programmer [left]

5.3 PocketQube Unit PCB

Unfortunately, not enough prototypes were ready for an end-project balloon launch. The power for the PQ unit was therefore implemented using large but readily available converters/regulators. In a final launch, this power section would either be replaced by the EPS or a low drop-out voltage regulator with a smaller LiPo. The PQ unit PCB was ordered through an external supplier. In order to begin initial development and testing, an Arduino Nano breadboard prototype was created, as shown in Appendix E.5. Since the Nano has the same MCU as the designed PCB, the developed software could then simply be flashed onto the PQ unit using an off-board programmer. The final module is shown in Figures 5.4 and E.11. As noted in the appendix errata, the crystal's loading capacitors were mistakenly left out. The MCU's internal 8 MHz clock was used, however was badly calibrated, and resulted in software serial communication with the GPS module not working. This was fixed by setting the OSCCAL register to calibrate the clock. The board was first bootloaded with an Arduino Nano, and then the programmer circuit in Figure 5.4 was developed to flash the board via UART. The programmer consists of a CH340 USB-to-serial module, a reset RC filter, as well as a 3.3V to 5V level converter (since the PocketQube PCB is designed to run at 3.3V). The board and dipole antenna was mounted onto the 2000 mAh LiPo battery. The power section consists of a LiPo charger, a boost converter module, and a 3.3V linear voltage regulator circuit.

5.4 PocketQube Unit Antenna

The PQ unit antenna was simply implemented using readily available 1.5 mm steel wire. The wire was bent by hand, and the end of u.FL pigtail cable was stripped and soldered to the wire. Lastly, insulation tape was added near the connection for stability and protection. The final design can be found in Figure 5.5.



Figure 5.5: PQ Unit Antenna Implementation

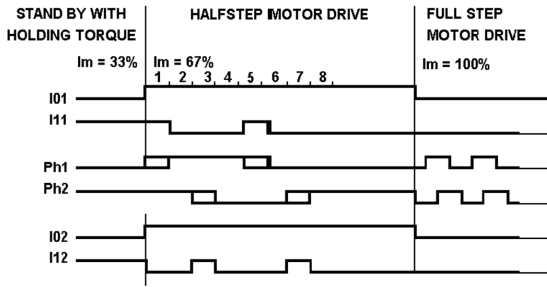


Figure 5.6: Stepper Motor Timing Diagram [6]

5.5 Software

All code is available at <https://github.com/gvcallen/pqcom/tree/main/code>.

5.5.1 Mount Control

The motors were setup in half-stepping mode, as shown in Figure 5.6, implemented using an array. Since both axes on the mount are dependent (see Figure E.1) the two-axis mount requires some relatively involved control. Elevational variation is straight-forward, as the azimuthal motor (controlled by Gear C) can be held fixed, and the elevation motor (Gear D) stepped accordingly. For azimuthal variation, if the elevation motor is held fixed, rotating the azimuthal motor causes the mount to also change in elevation, which must be compensated (demonstrated in Appendix E.3). The formulae to do this can be found in Appendix C.5. To smoothly step both motors simultaneously, speeds are then set according to the ratio of the number of azimuthal and elevation motor steps to do.

5.5.2 Pointing

A small library titled *wgs84* was used for the Mercator projection, with Cape Town as the origin. This allows a pointing vector to be determined, which is passed as the mount's boresight (where it is converted to azimuth-elevation co-ordinates). Unfortunately, the IMU (MPU-9250) was found to be counterfeit and lacked a magnetometer. The constraint was therefore made that a dead-reckoning fix to face magnetic north will be done. The angle between the zero sensor and magnetic north was therefore used as a reference input.

5.5.3 Radio and GPS

Existing Arduino libraries *RadioLib* and *TinyGPSPlus* were initially used for communication with the LoRa module and GPS module respectively. It was later found, however, that *RadioLib* was too large in program size for the Atmega328, and it was therefore replaced with *LoRaLib*, a smaller alternative.

6. Testing

6.1 Ground Station PCB

After implementation, initial tests were done to ensure the ground station was functional. This included ensuring all modules (radio, GPS and IMU) could be interfaced with successfully, as well as a few more detailed power tests, documented below.

6.1.1 Power

During no load from the motors, the voltage readings in Table 6.1 were obtained. The ESP and GPS lights were noted to be on. From these tests, it is clear that the full power system is working as expected. The current through a 12.3 V supply was measured at 179 mA i.e. 2.2 W power. Since a total of around 1 W of power is expected during no transmission (see Table D.1), this means that the voltage regulators are dissipating the remaining 1.2 W. This is well within the limitations of both regulators e.g. the LD1117 can dissipate a theoretical maximum of 12 W. The system was then left idle for an hour, with no noticeable change in current or heat.

Component	Expected	Measured
LD1117	3.3 V	3.307 V
LM7805	5 V	5.069 V
XL6009	24 V	24.07 V

Table 6.1: Ground Station Voltage Measurements

6.1.2 Motor Drive

The motor drive system was tested with the half-step sequence mentioned. Current measurements were made for different operating conditions and are listed in Table 6.2. Tests 1-4 were conducted using a *calibrate - return to stow* cycle repeated 10 times at 2/3 maximum current. The goal of these tests was to determine the speed limitations of the system, since it is easy to identify if the system misses steps, or if the gears slip, by moving it back and forth continuously. Tests 5-6 were conducted with the mount stationary at 75 degrees elevation with 2/3 and 3/3 current, respectively. These tests were intended to stress test the current handling and heat dissipation capabilities of the system. Note that the idle current of 179 mA was subtracted from each measurement.

Test No.	Description	I_{avg} (A)	Observation
1	40 ms step delay	0.7	No noticeable steps missed
2	20 ms step delay	0.7	No noticeable steps missed
3	10 ms step delay	0.56	Small slip near calibration start
4	5 ms step delay	0.25	Large number of steps missed
5	2/3 current; 1 hour	0.71	Minimal system change across the hour
6	3/3 current; 1 hour	2.1	Stabilised current but very hot mount

Table 6.2: Motor Drive Operating Tests @ 12 V supply

Since the boost converter operates as a DC transformer, the current consumed by the motor drive near the start of the hour can be calculated as $2.031 \times \frac{12}{24} \div 2 = 0.509$ A. This is slightly higher than the designed reference current of 475 mA, however it is assumed that the L6219 was dissipating the remainder, since it was observed to increase in temperature. Since the system is stable near the end of the hour, and the L6219 has thermal shutdown, the system is considered to be within a safe operating region, even though it is clear the power dissipated in the driver increased throughout the hour. Lastly, it should be noted that, although the stepper motors meet the torque requirements, it is clear that the mount's gear system was not designed for such a large load. Future projects should therefore consider a stronger design.

6.2 PocketQube Unit PCB

As mentioned, it was decided that a balloon satellite would not be flown by the E&E department. Therefore, integration with the other PocketQube modules was not prioritised for the PCB and the RS-485 line drivers were left off the board. Current consumption for the rest of the components, however, was measured at 31 mA when the system was directly powered from a power supply running at 3.3 V. This is only 6 mA lower than the total current expected from the GPS and MCU ICs, indicating conformance to the original design.

6.3 Ground Station Antenna

The ground station antenna's return loss was measured using a network analyser to ensure it was correctly matched to 50Ω . The resultant graph is shown in Figure 6.1. The figure shows that the simple matching strip design is effective and was implemented correctly, however it should be noted that the null is not as deep as simulated (only around -10 dB minimum at 427 MHz as opposed to the -35 dB simulated minimum at the centre frequency of 433 MHz). This may either be due to the aluminium foil used being far from

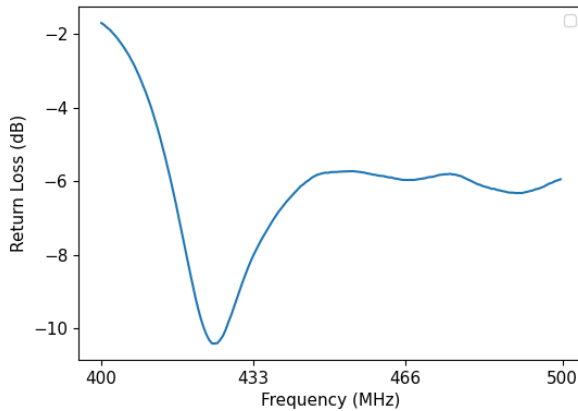


Figure 6.1: Measured Helical Antenna
Return Loss vs Frequency

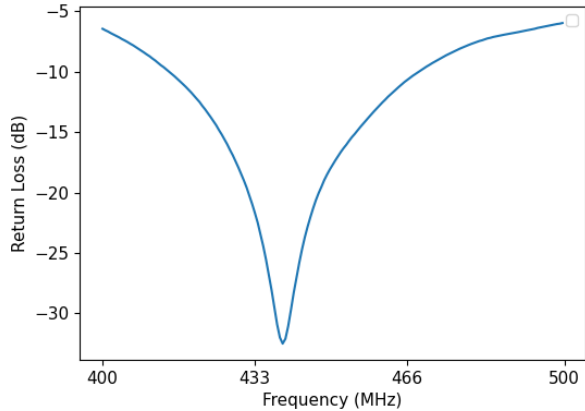


Figure 6.2: Measured Dipole Antenna
Return Loss vs Frequency

an ideal PEC, or most likely due to the imperfections in the antenna's construction (e.g. bends in the coil, the added dielectric resonance due to the PVC and wooden dowels etc.). Instead of optimizing the antenna build, however, it was decided to run further tests with the system as-is, since the link budget allows for up to a 1 dB matching loss. Optimisation is therefore left for future projects. Lastly, the antenna pattern unfortunately could not be measured, as a chamber was not available that could measure the desired frequency range.

6.4 PocketQube Unit Antenna

The return loss of the PQ dipole antenna is shown in Figure 6.2. It is clear that, due to the antenna's simple construction, the resulting match is near-perfect. Since frequencies from around 420 to 440 MHz provide less than 0.1 dB mismatch loss, the final system frequency can be chosen solely using the helical antenna's return loss graph.

6.5 RF Module

The radio modules were initially tested using two small, 433 MHz helical antennas. The first was placed near a window indoors, and the second inside a car. A range of 50 m was recorded in an urban area with a LoRa spreading factor of 8. This test served merely as a "proof-of-concept", and was not intended as an indication of system performance.

6.5.1 Transmit Power Consumption

The custom-built antennas were then connected to both the PQ and the GS and more detailed tests were conducted. The first test measured the power consumption for the PQ unit as a function of transmit power. This is displayed in Figure 6.3, after subtracting a 31 mA "no-transmit" current. The maximum current is around 96 mA for the maximum output power (quoted by the RA-02 as 18 dBm +- 1 dBm).

6.5.2 Data Rate

To test the possible bit rates as a function of LoRa spreading factor (SF), two RA-02 modules were setup with the same parameters and the bit rate was measured as the SF value was varied. A payload length of 255 was used, with 4/6 CRC, an 8 bit preamble, 500 kHz bandwidth, and a 10 ms delay between packets. The bit rate was then measured on the receiving side and is shown in Table 6.4. Theoretical bit rates were derived using the calculator at [31]. The results show that the system is set up correctly, and that a spreading factor of 8 is the correct choice to achieve the 9600 baud rate requirement.

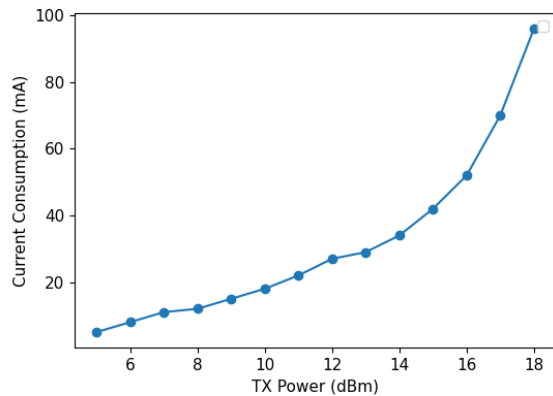


Figure 6.3: TX Output Power vs Current Consumption

Spreading Factor	Theoretical Bit Rate (bps)	Measured Bit Rate (bps)
7	18229	17200
8	10417	10240
9	5859	5800
10	3255	3320
11	1790	1846

Figure 6.4: LoRa Bit Rate vs Spreading Factor

6.6 GUI

The interface was tested to ensure that it met the desired functionality. An example of the output received on the GUI’s monitor is shown in Figure 6.5, after the calibration button was pressed; flight path data was uploaded; the tracking method was set to open-loop (“GPS Uploaded”); and the system was left for some time. Further outputs, as well as the whole interface, are shown in Appendix F.3.

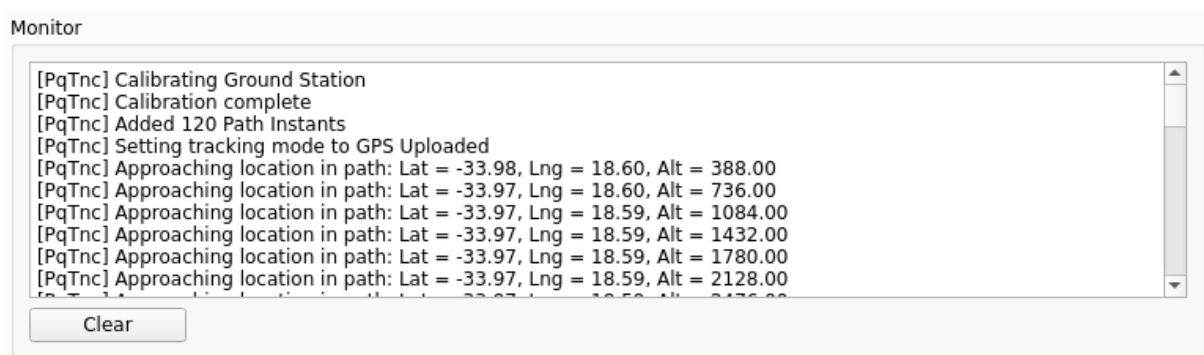


Figure 6.5: GUI Monitor after “Calibrate”, “Upload”, and “Set Track Mode”

6.7 Range

Line-of-sight range tests were conducted. Both antennas were manually positioned, and the PQ dipole was placed both horizontally and vertically. All measurements were done at the designed parameters i.e. SF 8, CR 4/6 and 500 kHz. The resulting *received signal strength indicator* (RSSI) and signal-to-noise (SNR) ratio was recorded. For the unfamiliar reader, the best theoretical RSSI is 0 dB, and the minimum SNR for SF 8 is -10 dB.

Tests were done in locations around the Western Cape, as described in Appendix F.2. The first test (not listed) was a 300 m test on Coetzenburg field in Stellenbosch. The link performance was found to be low compared to subsequent tests, with a recorded RSSI of -92 dBm. It is assumed that ground bounce was the major contributing factor.

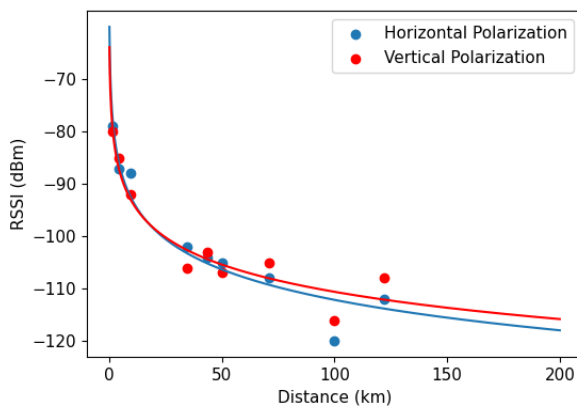


Figure 6.6: Measured RSSI vs Distance

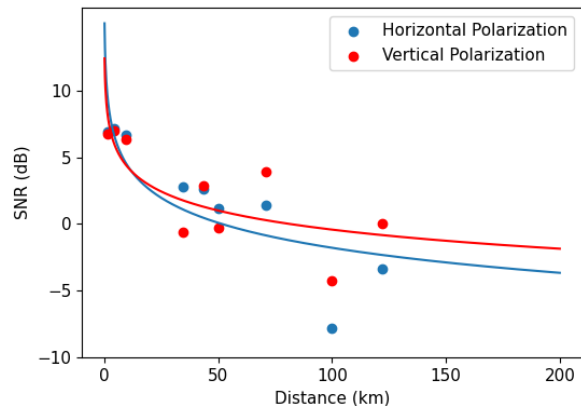


Figure 6.7: Measured SNR vs Distance

The results for the rest of the tests are plotted in Figures 6.6 and 6.7, with a logarithmic curve fit. The packet contents were verified using an ID, the transmitted GPS location, and by inspecting whether a CRC (Cyclic Redundancy Check) error had occurred. The system successfully met the 120 km range requirement, and a reliable link was established at the final test of 122 km, with a recorded RSSI of -108 dBm for the vertically polarized case. Although the SNR appears to be adjusted by the receiver at closer distances, the RSSI appears to follow a logarithmic curve well, as predicted by the free space path loss formula. All tests also had a 100% packet reception rate once in steady-state. For the required distance, at a sensitivity of -119 dBm, this indicates an 11 dB margin, which is slightly less than the final designed value of 12.8 dB. It is clear that the 100 km is an outlier, and is assumed that this was due to strong multi-pathing affects caused by the transmitter being sub-optimally placed with a large rock directly behind it.

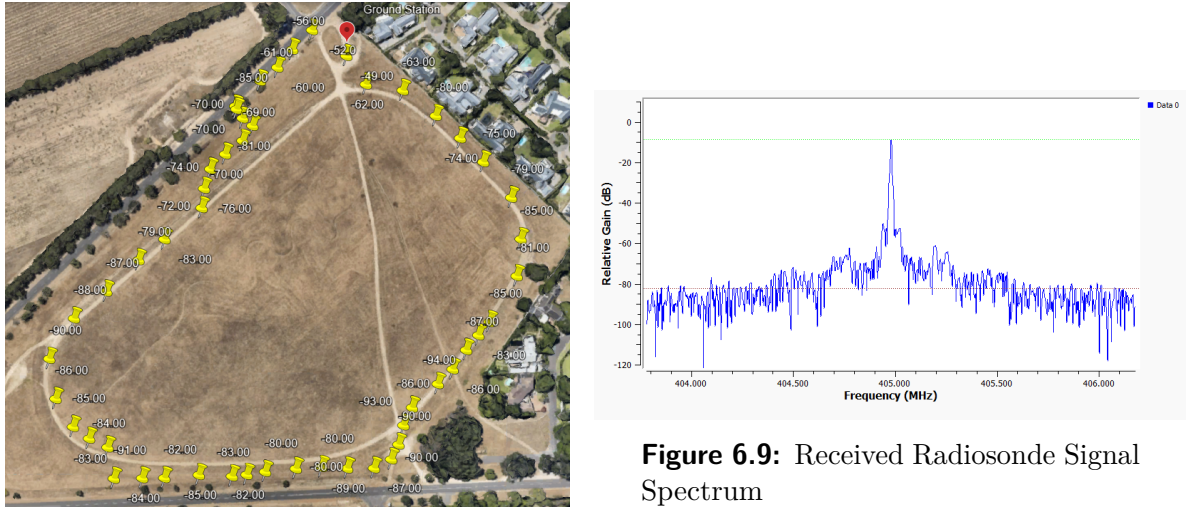


Figure 6.8: GPS Tracking Locations and RSSI Values

Figure 6.9: Received Radiosonde Signal Spectrum

6.8 Tracking and Pointing

6.8.1 Open-Loop

In order to test the GPS pointing and open-loop tracking, a map was printed with lines pointing to nearby locations from a pre-determined location. The ground station was then placed on top of this map at this location and calibrated (as described in Appendix D.8). This test had multiple goals i.e. to test the mount transfer function, the GPS co-ordinate pointing, and the flight path tracking. An image of the test setup is shown in Figure F.1.

Flight path data containing the map locations was then uploaded, and the azimuthal angle was qualitatively confirmed to point in the map directions using a ruler. The elevation angle was measured using a protractor and found to be within 5° of the expected angle. The system was also found to successfully point towards the commanded locations at the desired times. Since the beamwidth of the antenna is on the order of 60° , it was decided not to use a more accurate testing technique, since it is clear the system was functional at least within requirements.

6.8.2 Closed-Loop

Closed-loop GPS tracking was tested on an open field at 300 m range. The PQ unit was carried around the field at a walking speed of 2 m s^{-1} while transmitting its GPS location. Both the RSSI, and the antenna pointing direction, were recorded. The system was observed to successfully track the transmitter around the field without noticeable delay. The 90° turn created by the furthest ends of the field creates an approximate 500 m path, which was covered in 100 s. This results in a turning rate of around 0.9° , which meets the requirement of 0.015° . The tracking was observed to be successful until the target reached

a distance of around 10 m, where the pointing direction became unpredictable. This is attributed to the low accuracy of the GPS modules.

6.9 Radiosonde

The helical antenna was setup to receive signal from a testing iMet-54 radiosonde using the RTL-SDR USB dongle and an SMA-MCX adapter. A resultant one-second squelch signal shown in Figure 6.9 was observed. A free Python script *Auto-RX* [32] was found which caters for several radiosonde types. This was used to retrieve the GPS location successfully.

6.10 Full System

The South African Weather Service kindly granted permission to track their weather balloons, which have radiosonde payloads. This allowed for full system tests to be conducted, with focus on closed-loop tracking. A first test was conducted near the launch location (Cape Town International), where closed-loop tracking was tested. Although the system computer unfortunately lost power near the 25 km mark, it was observed that the mount correctly steered the antenna based on the received GPS data. The results of both the predicted path and the actual path for this test, as well as the recorded SNR as a function of distance, are shown in Figures 6.10 and 6.11. A second test was conducted from Constantia, around 17 km from launch. The mount correctly pointed towards the launch location using a predicted path, and received the radiosonde's GPS location when it reached an altitude of 5.1 km. Due to time constraints, the test was then concluded.

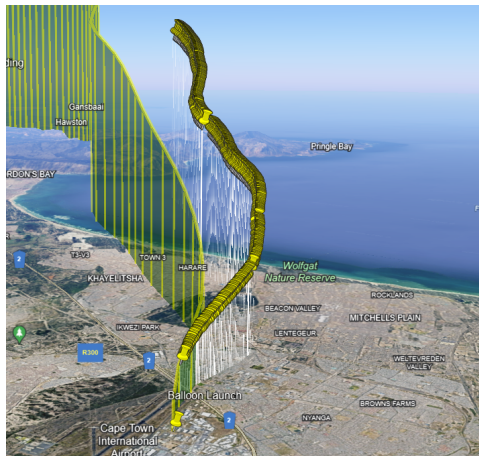


Figure 6.10: Radiosonde Closed-Loop Tracking Predicted Path (left) vs Actual (right)

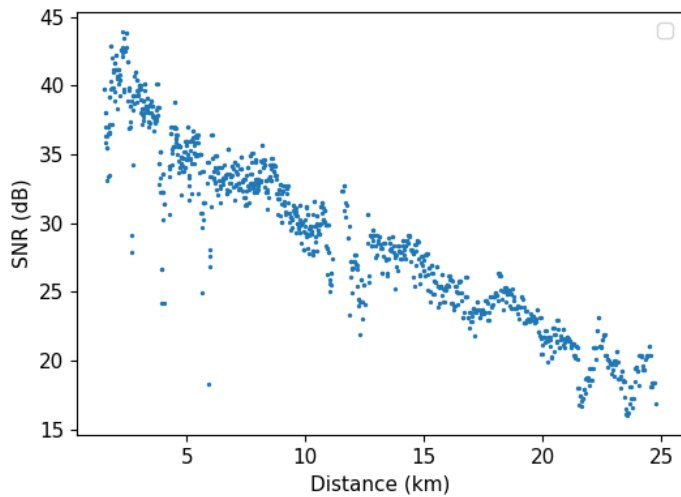


Figure 6.11: Radiosonde Closed-Loop Tracking SNR vs Distance

7. Conclusion

7.1 Summary

A PocketQube communication system, with a tracking ground station and a PocketQube PCB module, was successfully designed to meet the system requirements for a balloon satellite launch in Saldanha Bay. Unfortunately, the launch did not take place, however several modularized tests helped to prove that the system is fully functional and capable of communicating over the required distances.

LoRa proved to be a viable choice for the custom communication link. Not only did the link meet the throughput requirements of 9600 baud, but the system's range was successfully tested up to 120 km line-of-sight. Further, the increased immunity due to the spread-spectrum technology suggests that it should be made a priority choice for low-cost, low-power satellite communication links. The helical antenna design also proved to be effective in the context of the project, as it was easy to manufacture, and allowed the system to meet its requirements.

The open-loop tracking method was successfully implemented, however was not integrated into a full-system test. Closed-loop GPS tracking was successfully tested for a weather balloon launch up until a range of 25 km, and appeared to be the preferred tracking method for balloon satellite systems, since an initial GPS fix was easy to establish.

Lastly, the final ground station and PocketQube module PCB designs and implementations were shown to be effective, allowing a good foundation for future work.

7.2 Future Work

There are various improvements and alternative choices that can be explored in the context of the developed system:

- *Improved ground station PCB.* The ground station PCB was designed to use break-out boards, through-hole components, and modules for rapid development. Future designs could replace almost all components with surface-mounted ones, and remove break-out boards (e.g. the ESP32 board) to reduce cost, improve connection integrity, and allow more space for additional components.
- *Improved helical antenna construction.* The ground station antenna can be optimised, by constructing it using more rigid materials to stricter manufacturing tolerances. This would hopefully decrease any variance between the simulation and the implementation, and improve the matching and radiation pattern. A longer antenna

with higher gain could also potentially be implemented if similar materials are used, considering that the mass-distance product of the implemented antenna was under half of the theoretical maximum.

- *Automatic orientation detection.* Currently, the ground station uses a dead-reckoning fix, by requiring that it be pointed towards magnetic north, and that it is orientated flat. Further work could be done to make use of an IMU in order to allow the ground station to be rotated at any angle.
- *PocketQube antenna integration.* The antenna for the PocketQube was not designed to be deployable, but the half-dipole was shown to provide an effective proof-of-concept. For integration into final PocketQube models, options include a deployable antenna (e.g. with a foldable spring mechanism); using a higher frequency band; or using a much smaller but lower efficiency normal-mode helical antenna.
- *Radiosonde link optimisation.* A dedicated, more sensitive radiosonde receiver targeted at the meteorological band (as opposed to a generic software-defined radio) could be implemented. This might require an RF switch, but would provide the ability to change between the custom and radiosonde link in software.
- *Signal strength scanning.* Faster signal strength “conical” scanning could be explored. Although it was not investigated in this project (as a brute-force scan or open-loop estimate is generally sufficient to initially find the payload and receive its GPS location) the flexibility of tracking the payload using only its received radio signal may be beneficial.
- *PocketQube assembly.* Since a prototype for all the sub-systems of a PocketQube communication system have been designed and tested, integration within an actual PocketQube housing can be investigated, and an actual PocketQube satellite can become a reality.

Bibliography

- [1] rose.edu. (2018) RSC Cyber Students Fly High with High Altitude Balloon Launch. [Online]. Available: <https://www.rose.edu/content/news-events/news/2018/06-june/rsc-cyber-students-fly-high-with-high-altitude-balloon-launch/>
- [2] D. Slabber. (2023) Pocketcube Mechanical Interface.
- [3] H. A. Science. Tracking a Weather Balloon. [Online]. Available: <https://www.highaltitudescience.com/pages/tracking-a-weather-balloon>
- [4] C. R. A. Inc. (2022) How To Make a 433 MHz Yagi Antenna Design For A Long-range? [Online]. Available: <https://lcantennas.com/433-mhz-yagi-antenna-design-for-a-long-range/>
- [5] Wikipedia. (2023) Inverted-F Antenna. [Online]. Available: https://en.wikipedia.org/wiki/Inverted-F_antenna
- [6] STMicroelectronics. (1996) L6219 Stepper Motor Driver. [Online]. Available: <https://www.mantech.co.za/datasheets/products/L6219.pdf>
- [7] Celestis. What are the "Azimuth" and "Elevation" of a Satellite? [Online]. Available: <https://www.celestis.com/resources/faq/what-are-the-azimuth-and-elevation-of-a-satellite/>
- [8] P. J. Bevelacqua. (2022) Antenna Theory. [Online]. Available: <https://www.antenna-theory.com/>
- [9] Semtech. 137 mhz to 1020 mhz Low Power Long Range Transceiver. [Online]. Available: <https://www.semtech.com/products/wireless-rf/lora-connect/sx1278>
- [10] weather.gov. Weather Balloons. [Online]. Available: https://www.weather.gov/bmx/kidscorner_weatherballoons
- [11] Sondehub. Hab-Hub Flight Path Predictor. [Online]. Available: <https://predict.habhub.org/>

- [12] Ringbell. Distance to the Horizon Calculator. [Online]. Available: <http://www.ringbell.co.uk/info/hdist.htm>
- [13] Omni-Calculator. Radar Horizon Calculator. [Online]. Available: <https://www.omnicalculator.com/physics/radar-horizon>
- [14] Internet. imet-54. [Online]. Available: <https://internet.co/wp-content/uploads/iMet-54-403MHz-GPS-Radiosonde-Brochure-V5.7.pdf>
- [15] S. e. a. Speretta, *A Multi Frequency Deployable Antenna System for Delfi-PQ*. Proceedings of the International Symposium on Space Technology and Science, Fukui (Japan), 2019.
- [16] R. Israel. Mercator's Projection. [Online]. Available: <https://personal.math.ubc.ca/~israel/m103/mercator/mercator.html>
- [17] C. A. Balanis, *Antenna Theory: Analysis and Design*, 2nd ed. John Wiley Sons, 1997.
- [18] sgcderek. Helical Antenna Calculator. [Online]. Available: <https://sgcderek.github.io/tools/helix-calc.html>
- [19] D. G. K.-H. et al. (2015) A Compact Low-Profile Ring Antenna with Dual Circular Polarization and Unidirectional Radiation for Use in RFID Readers. [Online]. Available: <https://ieeexplore.ieee.org/stamp/stamp.jsp?arnumber=8822972>
- [20] J. Fernandez. (2018) Link Budget Calculation. [Online]. Available: <https://github.com/FOSSASystems/FOSSASAT-1/blob/master/FOSSA%20Documents/FOSSASAT-1%20Link%20Budget.pdf>
- [21] M. Arias. (2016) Small Satellite Link Budget Calculation. [Online]. Available: https://www.itu.int/en/ITU-R/space/workshops/2016-small-sat/Documents/Link_budget_uvigo.pdf
- [22] K. Cheung. The Role of Margin in Link Design and Optimisation. [Online]. Available: https://s3vi.ndc.nasa.gov/ssri-kb/static/resources/15-0025_A1b.pdf
- [23] I. Campbell Scientific. The Link Budget and Fade Margin. [Online]. Available: <https://s.campbellsci.com/documents/us/technical-papers/link-budget.pdf>
- [24] GOMspace. (2011) CubeSat Space Protocol (CSP).
- [25] E. E. Harstad. Analysis of Balloon Trajectory Prediction Methods. [Online]. Available: <https://www.iastatedigitalpress.com/ahac/article/8334/galley/7926/view/>

- [26] A. Wonggeeratikun, S. Noppanakeepong, N. Leelaruji, N. Hemmakorn, and Y. Moriya, *The Analysis of the Airplane Flutter on Low Band Television Broadcasting Signal*. ResearchGate, 2023.
- [27] L. Engineering. High Torque Motor. [Online]. Available: <https://cnctar.hobbycnc.hu/ZOTYK%C3%93/NEMA%2017%20motorom%20adatlapja%204218M-01.pdf>
- [28] Gravitech. (2014) Arduino Nano. [Online]. Available: https://www.arduino.cc/en/uploads/Main/Arduino_Nano-Rev3.2-SCH.pdf
- [29] everythingRF. Free Space Path Loss Calculator. [Online]. Available: <https://www.everythingrf.com/rf-calculators/free-space-path-loss-calculator>
- [30] J. Kraus and R. Marhefka, *Antennas for All Applications*, ser. McGraw-Hill series in electrical engineering. McGraw-Hill, 2002. [Online]. Available: <https://books.google.co.za/books?id=V6pSPgAACAAJ>
- [31] R. W. World. LoRa Data Rate Calculator. [Online]. Available: <https://www.rfwireless-world.com/calculators/LoRa-Data-Rate-Calculator.html>
- [32] projectchorus. Automatic Radiosonde Receiver Utilities. [Online]. Available: https://github.com/projectchorus/radiosonde_auto_rx

A. Project Plan

Week	Tasks
02 (31/07 to 06/08)	Initial research; component selection
03 (07/08 to 13/08)	System-level design; initial system layout; components ordered
04 (14/08 to 20/08)	PCB design without traces; initial circuit design
05 (21/08 to 27/08)	Component prototyping; Full PCB design; initial antenna design
06 (28/08 to 03/09)	Mechanical design; Custom link investigation; PCB ordered
07 (04/09 to 10/09)	Reporting
08 (11/09 to 17/09)	Initial build
09 (18/09 to 24/09)	Software design; initial testing
10 (25/09 to 01/10)	Software design; debugging
11 (02/10 to 08/10)	Reporting
12 (09/10 to 15/10)	Design improvement
13 (16/10 to 22/10)	Testing
14 (23/10 to 29/10)	Reporting
15 (30/10 to 05/11)	Reporting

Table A.1: Initial Project Plan

B. Outcomes Compliance

Outcome	Description of Outcome in Report	Chapter(s)
ELO 1. Problem Solving	The project required developing a tracking satellite ground station with various constraints. The requirements and specifications had to be formulated in the project. The size and power constraints of both the ground station and the PocketQube unit had to be considered. The mount had mechanical limitations, such as the physical size of the antenna that it could support, which presented a problem to be solved.	Chapters 1, 3 and 4
ELO 2. Application of scientific and engineering knowledge	The design of the ground station and antenna system incorporated engineering knowledge from various fields, such as electromagnetic theory; telecommunications theory; computer systems; computer programming; and controls systems. Finally, skills required for a higher-level systems design were also needed.	Chapters 3, 4, 5, 6
ELO 3. Engineering Design	The waterfall design approach was followed. First, a systems-level design was conducted to determine the required functionality of the system. Then, engineering design was done for each sub-system, which includes circuit and PCB design; antenna design and software design.	Chapters 3 and 4
ELO 4. Investigations, experiments and data analysis	Hardware prototyping and testing was done on a breadboard to investigate the capabilities of the hardware, before implementing the final system. Various tests were then done on the final system, such as antenna measurements; long-range signal strength measurements; and GPS tracking tests. The results from these tests were analysed to determine if the system met the original requirements.	Chapters 5 and 6

Table B.1: ECSA Outcomes Compliance 1

Outcome	Description of Outcome in Report	Chapter(s)
ELO 5. Engineering methods, skills and tools, including Information Technology	PCB Design software <i>KiCAD</i> was used to design the PCBs. Electromagnetic CAD software <i>FEKO</i> was used for the antenna design and simulation. The <i>PlatformIO IDE</i> along with the <i>Arduion Framework</i> and the <i>C++</i> language were used to implement the software. Finally, <i>Python</i> was used for data analysis.	Chapters 4, 5 and 6
ELO 6. Professional and technical communication	The final report is written in the appropriate format, structure, and formal language in order to communicate the report's findings. It was written in Latex, which is thoroughly used in professional and technical communication.	
ELO 8. Individual work	The design, implementation and testing of the project was conducted entirely by the student, except for supervision from the lecturer.	
ELO 9. Independent Learning Ability	The project requirements were drawn up independently given loose requirements. The antenna design techniques, tracking methodologies, simulation environments, and PCB design skills were independently researched throughout the course of the project. Further, the relevant mechanical knowledge, such as the stepper motor drive and the antenna manufacturing, was acquired independently through problem-solving and research.	

Table B.2: ECSA Outcomes Compliance 2

C. References

C.1 PQSU

Pocketcube Mechanical Interface

Dirk Slabber, MEng | Electronic Systems Laboratory | Stellenbosch University

13/06/2023

* unless otherwise specified all measurements are to “The PocketQube Standard” [Issue 1, 7th of June, 2018], PQ9 and CS14 standard.

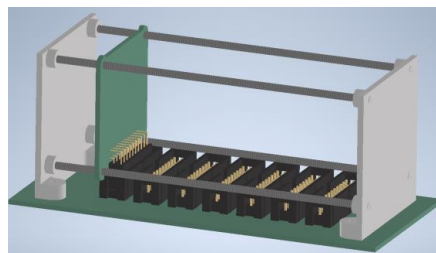


Figure 1- pocketcube structure

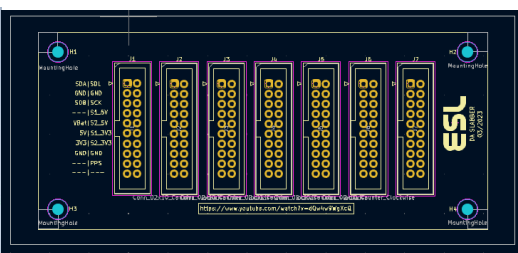


Figure 2- pocketcube bus layout

Physical Envelope

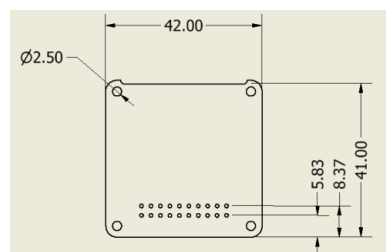


Figure 3-dimensions of the slot

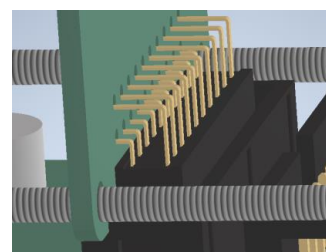


Figure 4-90-degree pins

Please take care to not place components such that it will obstruct the 90-degree bus pins as well as the nuts that will hold the slot in place around the four mounting holes. Components may project up to 8mm away from the board and still slot in with another board directly next to it.

Electrical Connection

Each slot is has twenty pins connected a bus in the main plate. Pin 1 is located top right on figure 3, pin 11 bottom right and so on. The suggested pinout on the bus is as follows:

1	SDA	SDL	11
2	Ground	Ground	12
3	SDB	System Clock	13
4	User defined	5V Switch 1	14
5	Power source	5V Switch 2	15
6	5V line	3.3V Switch 1	16
7	3.3 line	3.3V Switch 2	17
8	Ground	Ground	18
9	User defined	PPS	19
10	User defined	User defined	20

C.2 SUNCQ

SUNCQ Protocol

Commands

The following lists all commands from TNC to host and vice-versa. The command reservations are:

- 0x00 to 0x2F Host-to-TNC DO commands
- 0x30 to 0x5F Host-to-TNC SET commands
- 0x60 to 0x7F Host-to-TNC GET commands
- 0x80 to 0x9F TNC-to-Host STATUS replies
- 0xA0 to 0xCF TNC-to-Host DATA replies
- 0xD0 to 0xFE Reserved
- 0xFF Invalid

Code	Name	Function	Payload	Bytes	Comments
0x00	RESET	Reset the system	-	0	
0x01	CALIBRATE	Calibrate the system	-	0	Full calibration e.g. ground station and all sub-systems
0x02	RETURN_TO_START	Return the system to its starting state.	-	0	The starting state is post-calibration.
0x03	RETURN_TO_STOW	Return the system to its stow state.			The stow state is pre-calibration. Typically used before system shutdown
0x30	SET_TNC_MODE	Enter a TNC mode	See <i>TNC_MODE</i>	1	
0x31	SET_TRACK_MODE	Set tracking mode	See <i>TRACK_MODE</i>	1	
0x32	SET_PATH_DATA	Upload flight path data	CSV file. See <i>Flight Path Data</i> .	Any	The payload length is provided as the first 8 bytes.
0x33	SET_POINT_DIRECTION	Set the direction that the mount should point at			Only applicable when no tracking mode is selected
0x60	GET_SIGNAL_RSSI	Get RSSI of the signal	-	0	
0x61	GET_LOCATION	Get location of the ground station	Lat;Lng;Alt (f32:f32:f32)	12	
0x80	TNC_STATUS	Sent by the TNC as an ACK or status alert.	See <i>STATUS_CODE</i> .	1	Status 0x00 is used as an "ACK" command.
0x81	TNC_MESSAGE	Sent by the TNC to communicate a String message to the host.	char[]	Any	A newline character terminates the message
0xA0	SIGNAL_RSSI	Response to <i>GET_SIGNAL_RSSI</i>	float	4	
0xD0-0xFE	RESERVED	Reserved			Reserved for future use
0xFF	INVALID	Invalid			For internal use

Details

TNC_MODE

Value	Description
0x00	Normal mode
0x01	KISS mode. This mode is exited using the KISS 0xFF command.

TRACK_MODE

The tracking mode is a combination flag i.e. multiple bits can be ORed together to specify that the payload must be tracked using multiple methods at once.

Value	Description
0x00	No tracking. Mount can be moved by setting the pointing vector.
0x01	Use uploaded GPS data
0x02	Use received GPS data (from payload)
0x04	Use signal strength, but only for an initial scan
0x08	Use signal strength, with dynamic conical scanning

STATUS_CODE

The following is a list of status codes that might be sent from the TNC to the host:

Value	Description
0x00	Acknowledge
0x01	Payload tracking unsuccessful/payload lost

Flight path data

Flight path data can be uploaded in the form of a little-endian binary stream (i.e. each field should be least significant byte first). The first field is a 2-byte number indicating the number of flight path instances to follow. Then, the fields below should be provided. Such a file can be generated by predicting a flight path at <https://predict.sondehub.org/>, generating a CSV file, and then using the data to generate a binary stream. In the current implementation, only 200 entries are catered for – if longer flights are needed, then multiple streams should be sent from the host intermittently. Time should be in Unix time (seconds since Epoch).

Name	Type
Time	uint64
Latitude	float32
Longitude	float32
Altitude	float32

C.3 Antenna Comparison

Type	Gain (dBi)	Beamwidth	Bandwidth	Size	Polarization
0.5λ Dipole	2.15	Omni-directional	Medium	Medium	Linear
Monopole	5.15	Omni-directional	Small	Small	Linear
Helical	< 20	Either	Large (50 - 60%)	Small-Medium	Circular
Microstrip	< 10	Either	Small-Medium	Small	Either
Yagi-Uda	< 40	Uni-directional	Small	Large	Linear

Table C.1: Qualitative Comparison of Antenna Characteristics [8]

C.4 Link Configuration Summary

Description	Modulation	Parameters	Bit Rate	Sensitivity
Maximum Bit Rate	GFSK	62.5 kHz	250 000 bps	-92 dBm
High Bit Rate	GFSK	40 kHz	38400 bps	-109 dBm
Target Bit Rate ($\approx 9600\text{bps}$)	GFSK	5 kHz	4800 bps	-115 dBm
-	LoRa	500 kHz, SF 8	10417 bps	-119 dBm
Maximum Sensitivity	LoRa	62.5 kHz, SF 12	24 bps	-147 dBm

Table C.2: Notable SX1278 Configurations [9]

C.5 Mount Control

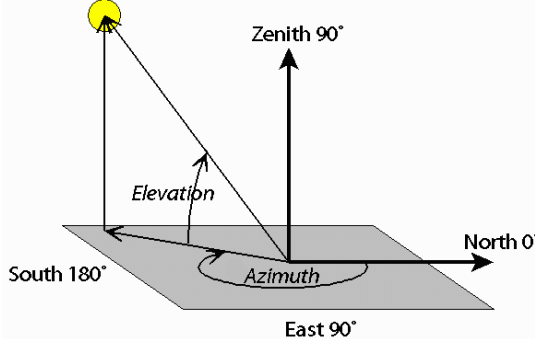


Figure C.1: Azimuthal and Elevation Visualization [7]

The “azel” ratio is the number of elevation motor turns required to tilt the elevation axis the same amount as the azimuthal motor, given by:

$$\text{azelRatio} = \frac{D_{\text{outer}}/B}{C/A} = \frac{92/20}{60/15} = 1.15 \quad (\text{C.1})$$

The azimuthal and elevation angles can then be calculated as in Formulae C.2 and C.3, where *elRev* and *azRev* are the number of elevation/azimuth motor steps per full revolution (equal to $200 \times \frac{92}{20} \times \frac{140}{80} = 1610$ and $200 \times \frac{60}{15} = 800$ respectively).

$$\text{azAngle} = \text{azPos} \times \frac{360^\circ}{\text{azRev}} \quad (\text{C.2})$$

$$\text{elAngle} = (\text{azPos} \times \text{azelRatio} + \text{elPos}) \times \frac{360^\circ}{\text{elRev}} \quad (\text{C.3})$$

The number of simultaneous “*delta*” steps to make in order for each axis to move to a new location {*newAzAng*, *newElAng*} implemented in *setAzimuthElevation()* is then given by Formulae C.4 and C.5.

$$\text{deltaAzSteps} = \text{angToPosAz}(\text{newAzAng}) - \text{azPos} \quad (\text{C.4})$$

$$\text{deltaElSteps} = -\text{deltaAzSteps} \times \text{azelRatio} + \text{angToPosDeltaEl}(\text{newElAng} - \text{elAng}) \quad (\text{C.5})$$

D. Design

D.1 Power Calculations

Component	Voltage	Current	Power
Motors	24 V	0.5 A (x4)	48 W
Motor Drivers	5 V	89 mA (x2)	890 mW
ESP32 Dev Board	5 V	120 mA	660 mW
RA-02	3.3 V	100 mA	330 mW
ATGM332D-5N31	3.3 V	25 mA	82.5 mW
MPU-9250	3.3 V	3.7 mA	12.21 mW
Total			49.97 W

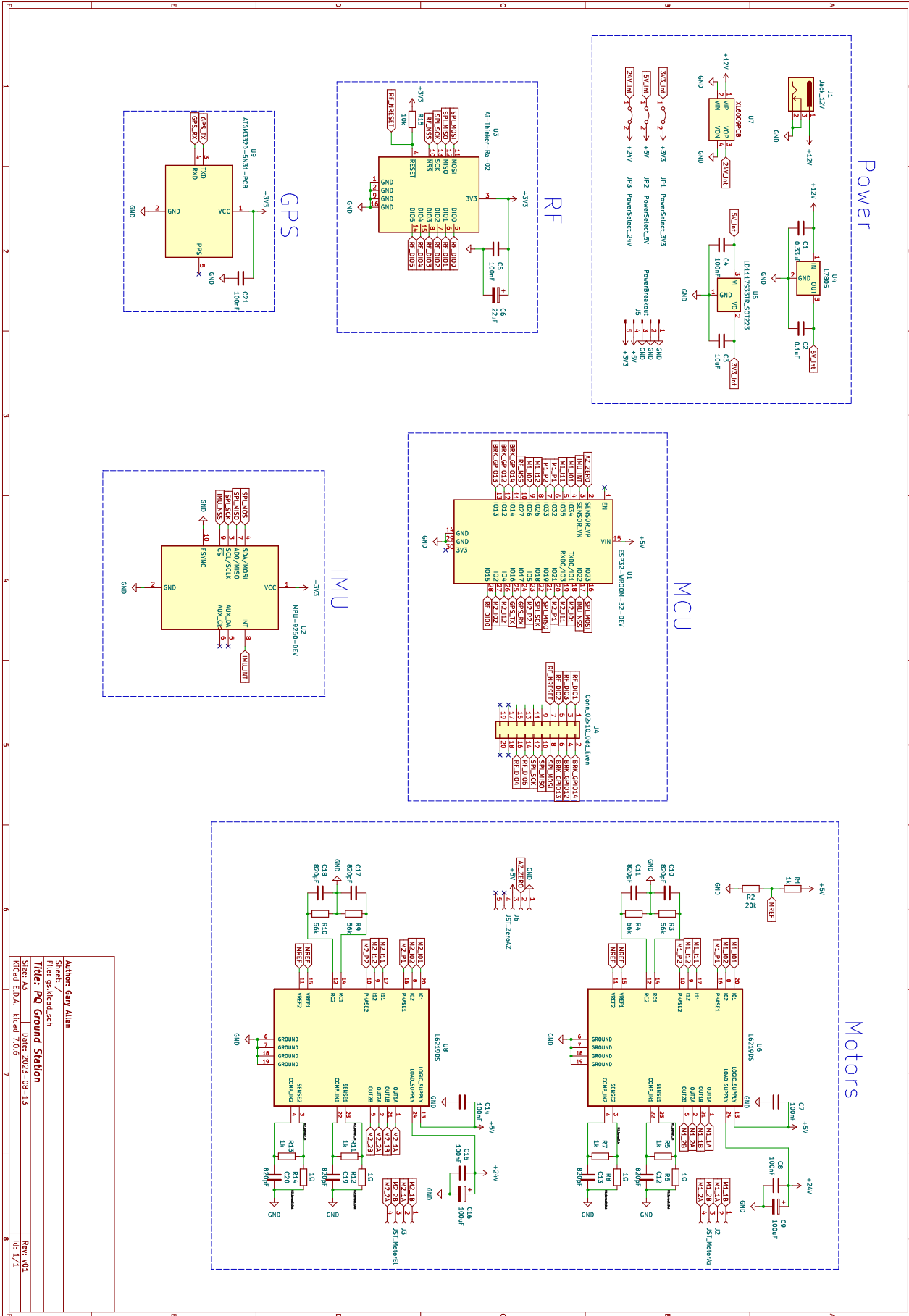
Table D.1: Ground Station Total Power Calculation

Component	Current	Power (@ 3V3)
ATmega328	12 mA	39.6 mW
RA-02	100 mA	330 mW
ATGM332D-5N31	25 mA	82.5 mW
MAX485	137.3 mA	1.0 mW
Total		453.1 mW

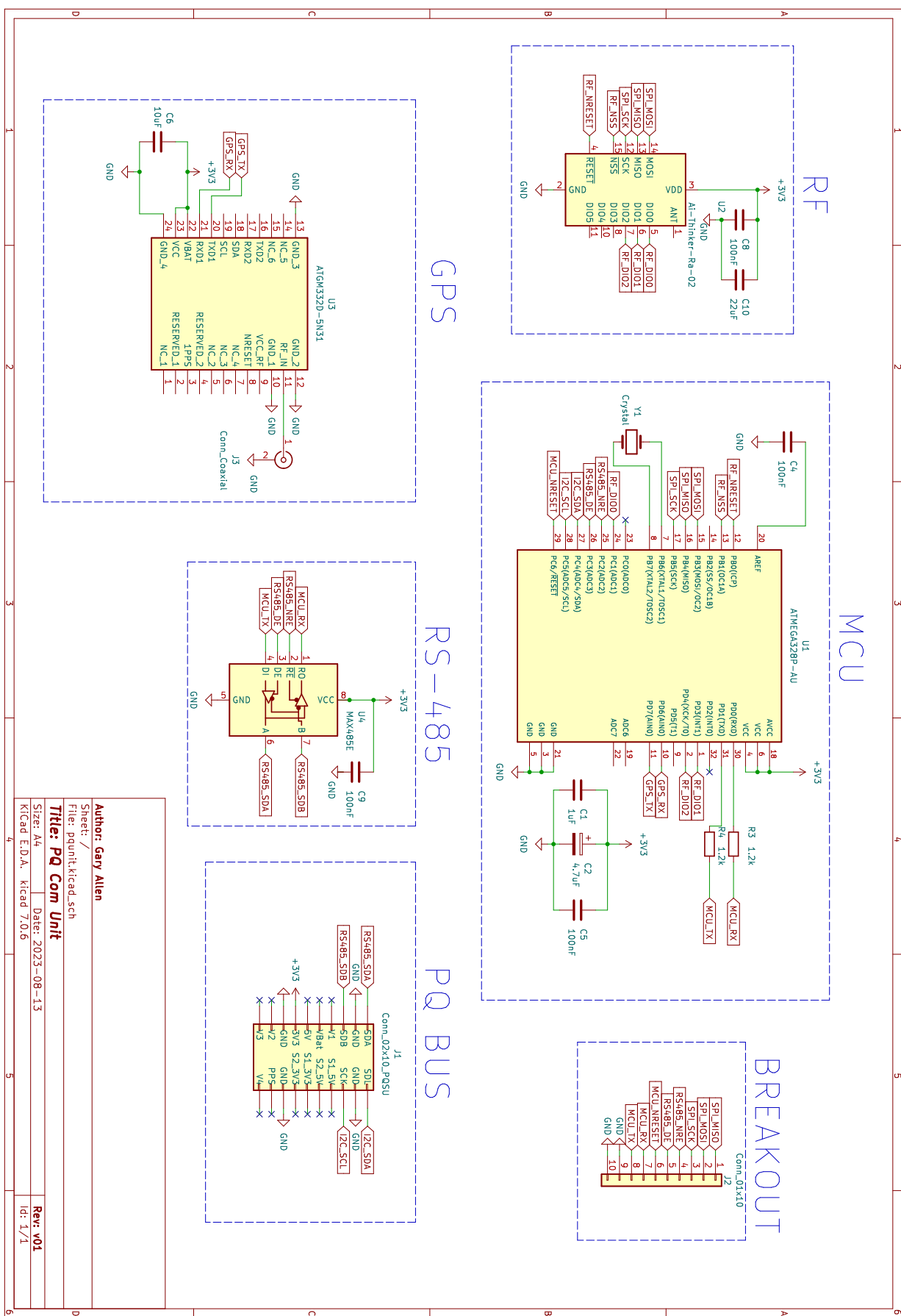
Table D.2: PocketQube Unit Component Power Consumption

D.2. Ground Station Schematic

D.2 Ground Station Schematic



D.3 PocketQube Unit Schematic



D.4 Ground Station PCB

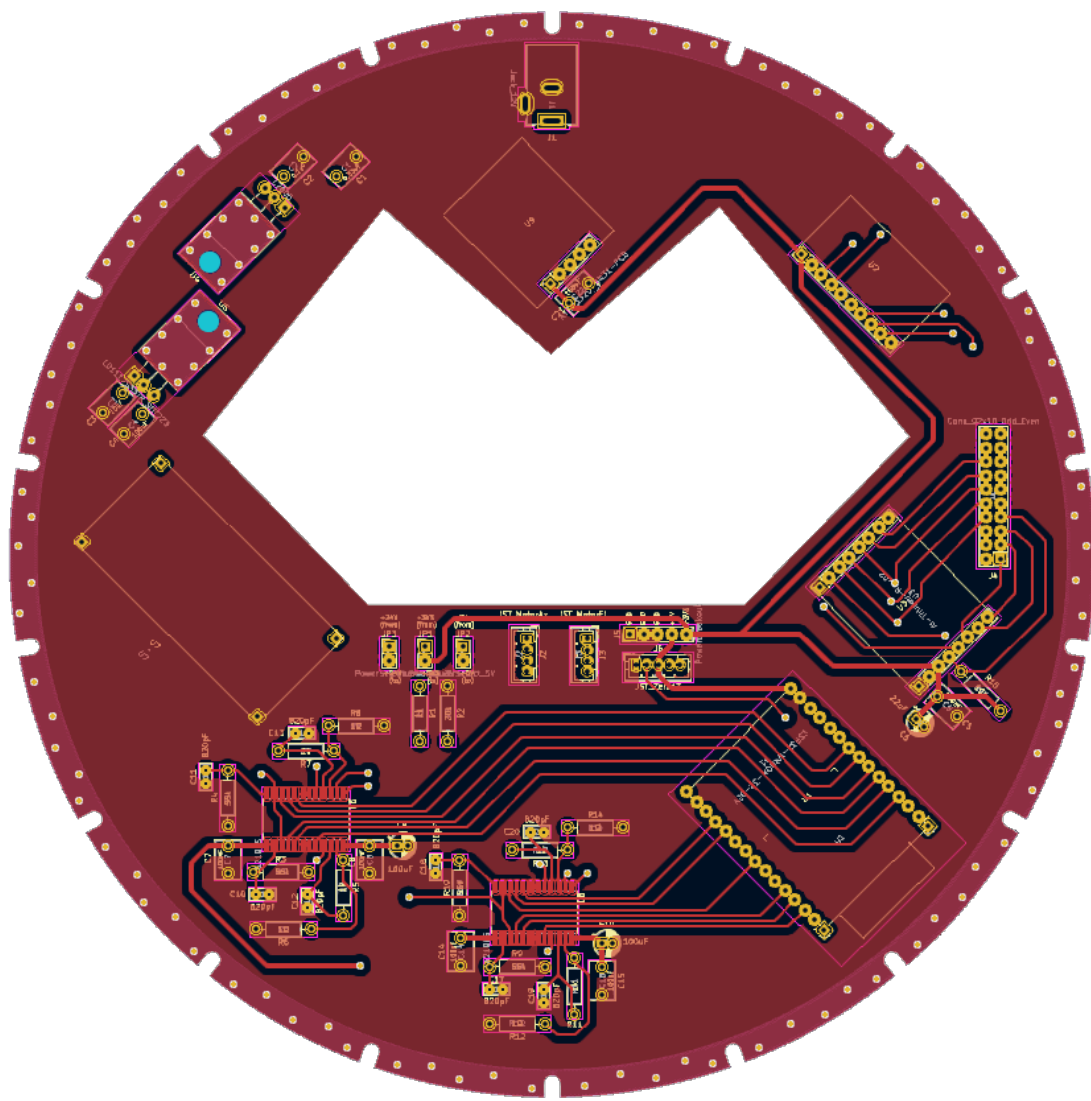


Figure D.1: Ground Station PCB Design (front)

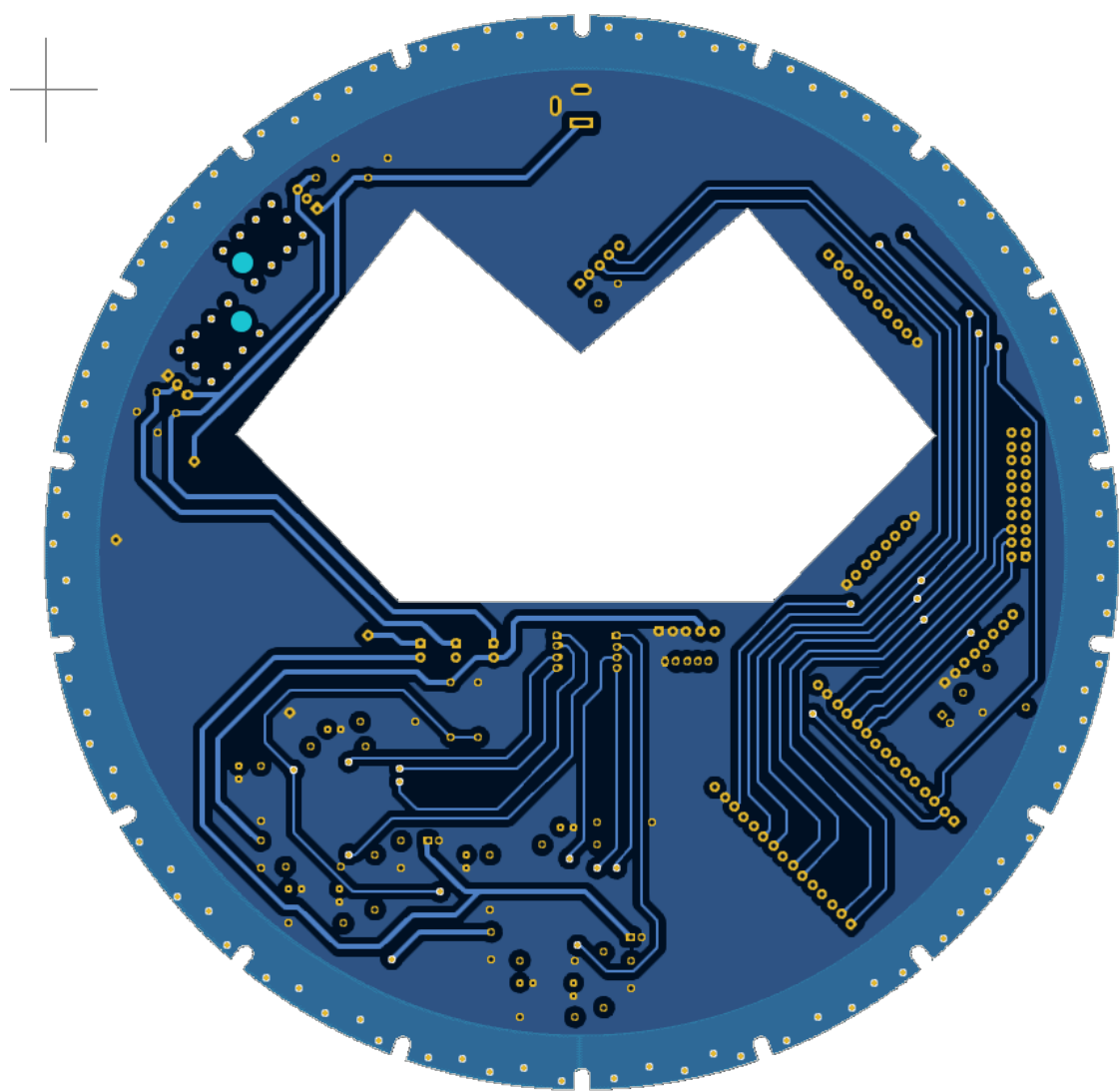


Figure D.2: Ground Station PCB Design (back)

D.5 PCB Errata

Ground Station PCB:

- The zero-sensor JST pin connections were incorrect.
- ESP Pins IO1 and IO3 should be left free for UART communication. Nets M2_IO1 and M2_I11 are therefore moved to pins IO14 and IO12 respectively.
- ESP Pins IO34 and IO35 are input-only. Nets M1_I01 and M1_I11 are therefore moved to pins IO0 and IO16 respectively. In this case, GPS_TX is no longer used, and pin 0 on-board the ESP module on the board must be soldered to directly.
- The ESP development board's footprint was sized slightly to wide, and should be narrowed to avoid having to bend the pins.

PocketQube Unit PCB:

- The loading capacitors on the crystal oscillator were incorrectly left out. The 8 MHz clock was therefore used, however the capacitors should be added in order for a 16 MHz clock to be used.

D.6 Ground Station Antenna

Parameter	Value
Diameter (D)	187.1 mm
Turn Spacing (S)	88.2 mm
No. of Turns (n)	4
Ground plane diameter (G)	> 350 mm
Strip height (sh)	19.4 mm
Strip width (sw)	77.7 mm
Strip length (sl)	132 mm
Cup height, if used (ch)	88.2 mm

Table D.3: Helical Antenna Final Parameters

D.7 Software

Table D.4: GPS Class

Function	Description
getLocation()	Return latitude, longitude and altitude
getTime()	Return seconds since epoch

Table D.5: Radio Class

Function	Description
startTransmit(message)	Transmit data (non-blocking i.e. with callback)
startReceive()	Start listening to receive data (non-blocking i.e. with callback)
getRssi()	Get signal strength
getSnr()	Get signal-to-noise ratio

Table D.6: Link Class

Function	Description
setTelemetryCallback(fn)	Set the "telemetry sent/received" function
setTelecommandCallback(fn)	Set the "telecommand received" function (<i>Responder</i> only)

Table D.7: StepperMotor Class

Function	Description
stepForward(numSteps)	Blocking and non-blocking options
saveZeroPosition()	Used for calibration
getPosition()	Used for open-loop feedback
setSpeed()	Sets the delay between steps
setCurrentMultiplier()	Set the amount of current

Table D.8: Mount Class

Function	Description
calibrate()	Calibrate the mount
setAzimuthalElevation(az, el)	Set the azimuthal and elevation angles
setBoresight(bore sightVec)	Set the boresight pointing vector

Table D.9: GroundStation Class

Function	Description
calibrate()	Calibrate the entire GS
addEstimatedLocation(loc)	Add an estimated input GPS location for open-loop tracking
addKnownLocation(loc)	Add a known GPS location for closed-loop tracking

D.8 Mount Calibration

The calibration procedure of the mount is described below:

- Measure the elevation angles of the mount at both extremes.
- Measure the offset angle between the zero-sensor and the desired magnetic north location.
- Lookup the magnetic declination near the area of interest.
- Include the previous three values statically in the software code.
- Rest the mount on the side with the larger elevation angle.
- Face the mount towards magnetic north.
- Run the mount's software calibration procedure, which rotates in azimuth until the zero sensor is found; then in elevation (open-loop) until the start elevation angle is reached; and finally faces north using the magnetic declination and offset angle.

E. Hardware

E.1 Mount Gears

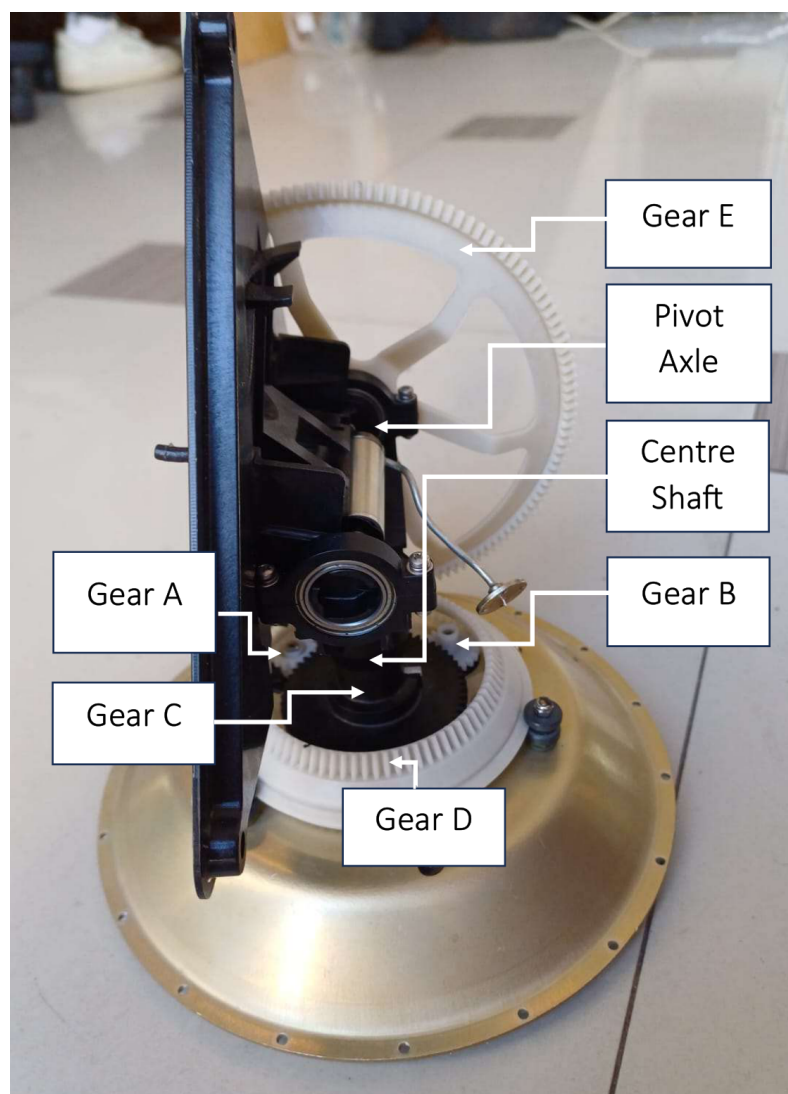


Figure E.1: The Existing Antenna Mount

E.2 Mount Specifications

Component	Specification
Motor	200 full steps (per 360 degrees)
Gear A	15 teeth
Gear B	20 teeth
Gear C	60 teeth
Gear D	92 inner teeth, 80 outer teeth
Gear E	140 teeth (equivalent)

Table E.1: Mount Gear and Motor Specifications

E.3 Mount Rotation



Figure E.2: Mount Azimuthal Compensation 1 (Elevation Fixed)



Figure E.3: Mount Azimuthal Compensation 2 (Elevation Fixed)



Figure E.4: Mount Azimuthal Compensation 3 (Elevation Fixed)

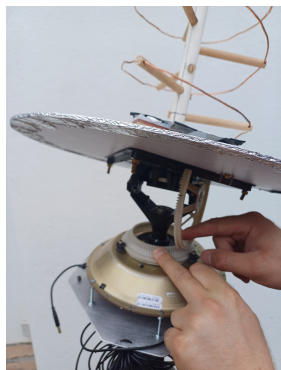


Figure E.5: Mount Azimuthal Compensation 4 (Elevation Fixed)



Figure E.6: Mount Azimuthal Compensation 5 (Azimuth Fixed)



Figure E.7: Mount Azimuthal Compensation 6 (Azimuth Fixed)

E.4 Existing Mount PCB

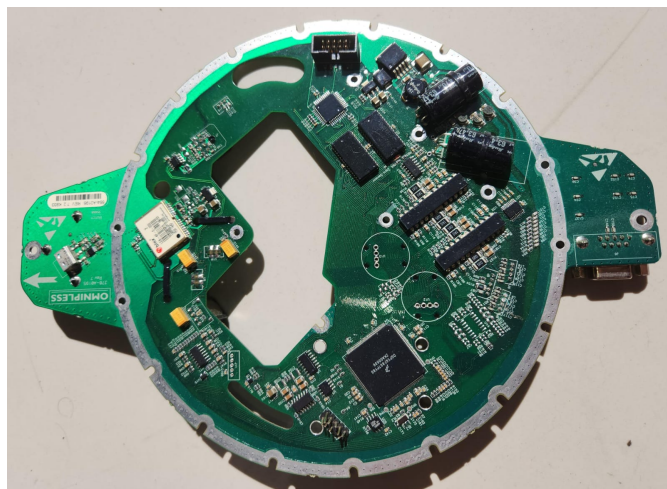


Figure E.8: Existing Antenna Mount PCB (front)

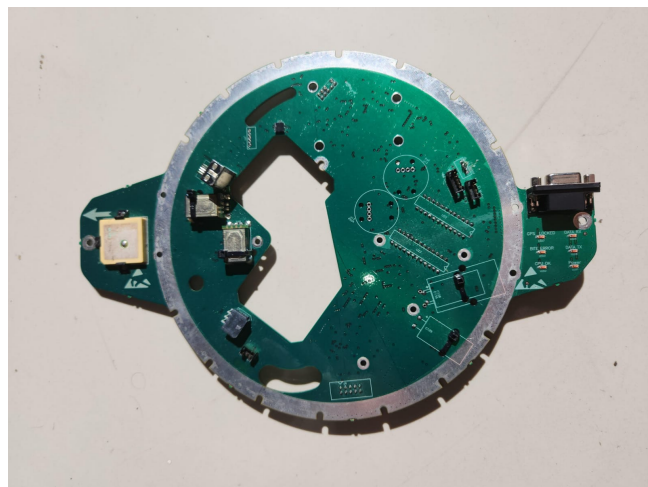


Figure E.9: Existing Antenna Mount PCB (back)

E.5 PocketQube

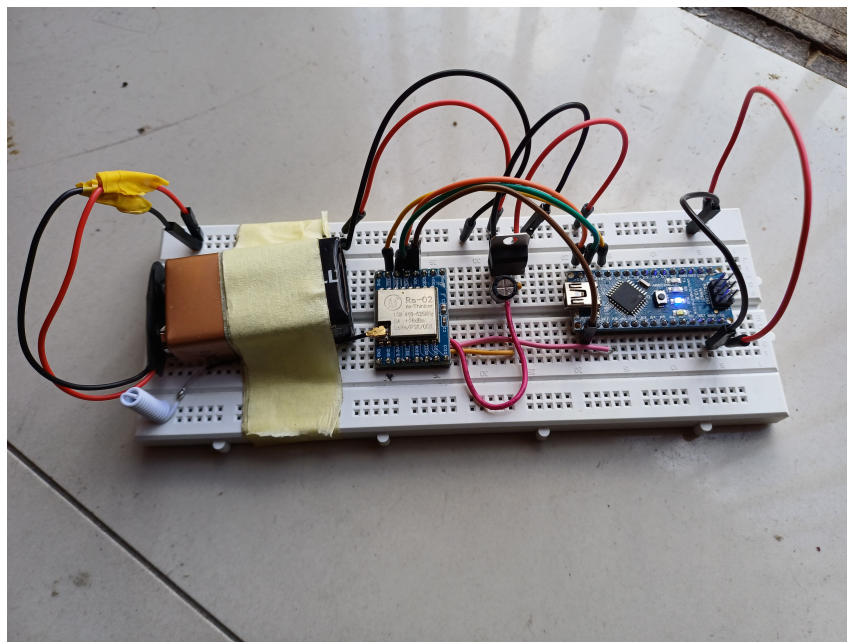


Figure E.10: PocketQube Breadboard for Testing

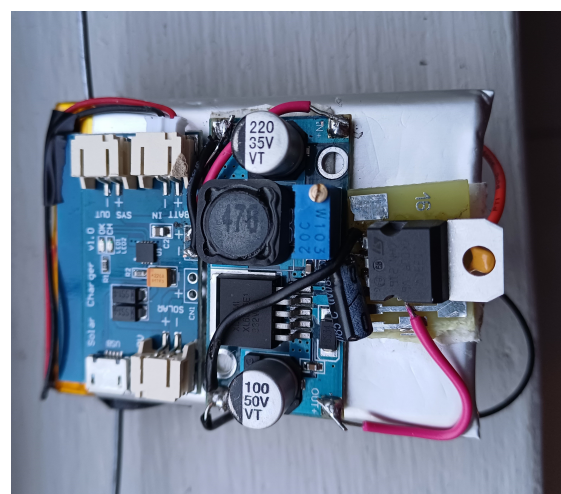


Figure E.11: PocketQube Unit (back)

F. Tests

F.1 Open-Loop Pointing Test



Figure F.1: Open-Loop Pointing Test Setup

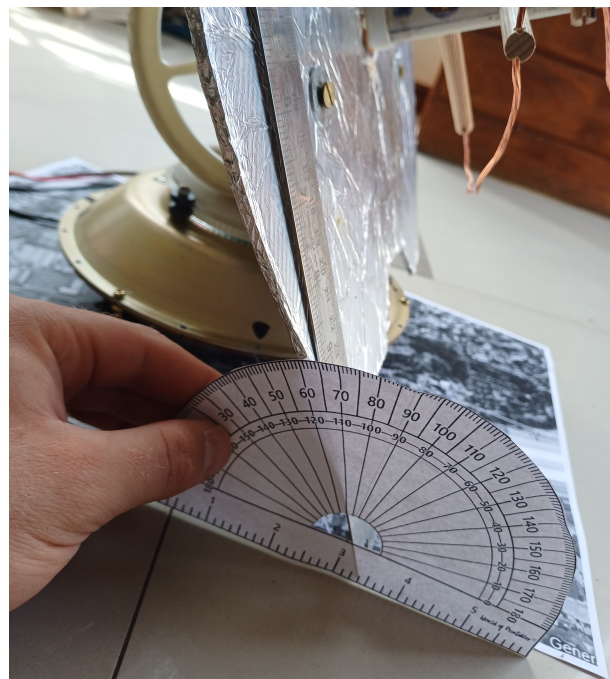


Figure F.2: Open-Loop Pointing Test Elevation Angle Measurement

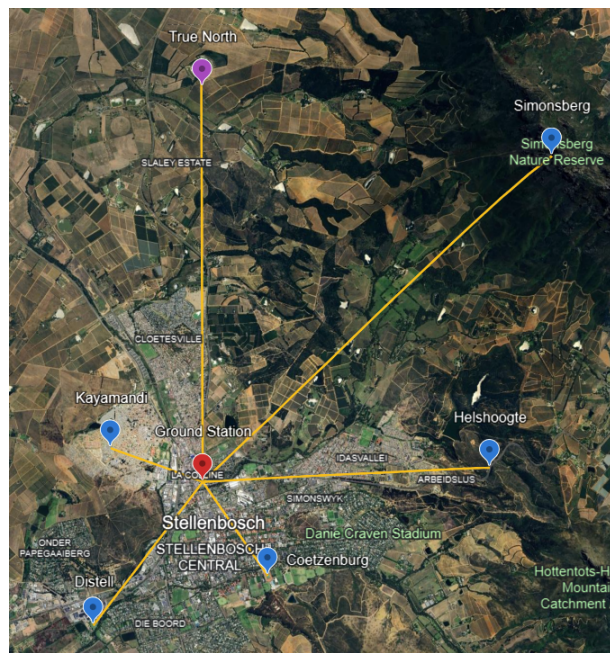


Figure F.3: Open-Loop Pointing Test Locations

F.2 Range Tests

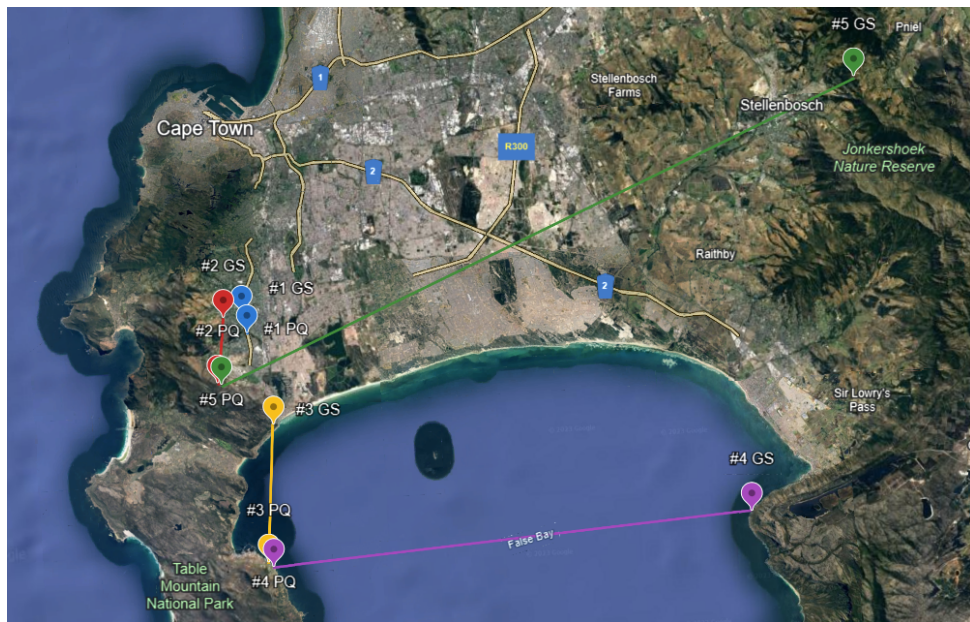


Figure F.4: Range Tests Mapped Locations 1-5

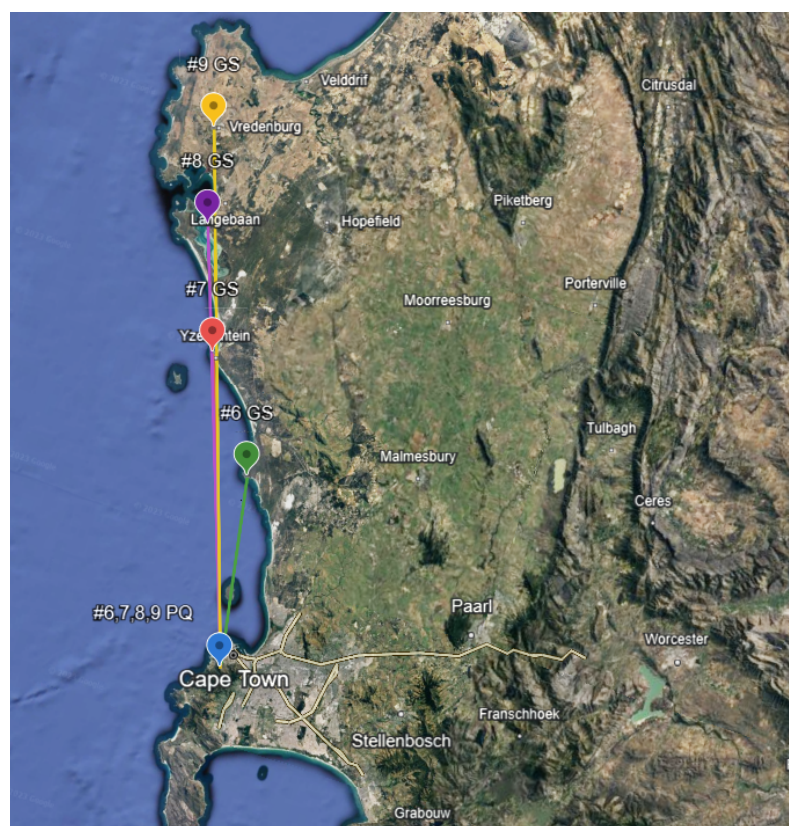


Figure F.5: Range Tests Mapped Locations 6-9

Test No.	Range	GS Location	PQ Location	Comments
1	1.4 km	Firgrove Way Bridge, Constantia	M3 Bridge near Keyser River	
2	4.6 km	Firgrove Way Field, Constantia	Silvermine	Cloudy conditions
3	9.7 km	Boys' Drive, Muizenberg	Windmill Beach, Simon's Town	
4	34.5 km	Steenbras Lookout	Windmill Beach, Simon's Town	
5	49 km	Tokara, Stellenbosch	Silvermine Lookout Point	Optimal transmitter placement uncertainty
6	43 km	Bokbaai	Table Mountain	
7	70 km	Schaap Island, Yzerfontein	Table Mountain	
8	100 km	Stompneus Lookout, Langebaan	Table Mountain	Sub-optimal transmitter placement (high multi-path effects observed)
9	122 km	Rock near Frans Koch Ave, Vredenburg	Table Mountain	

Table F.1: Range Test Location Descriptions

F.3 GUI

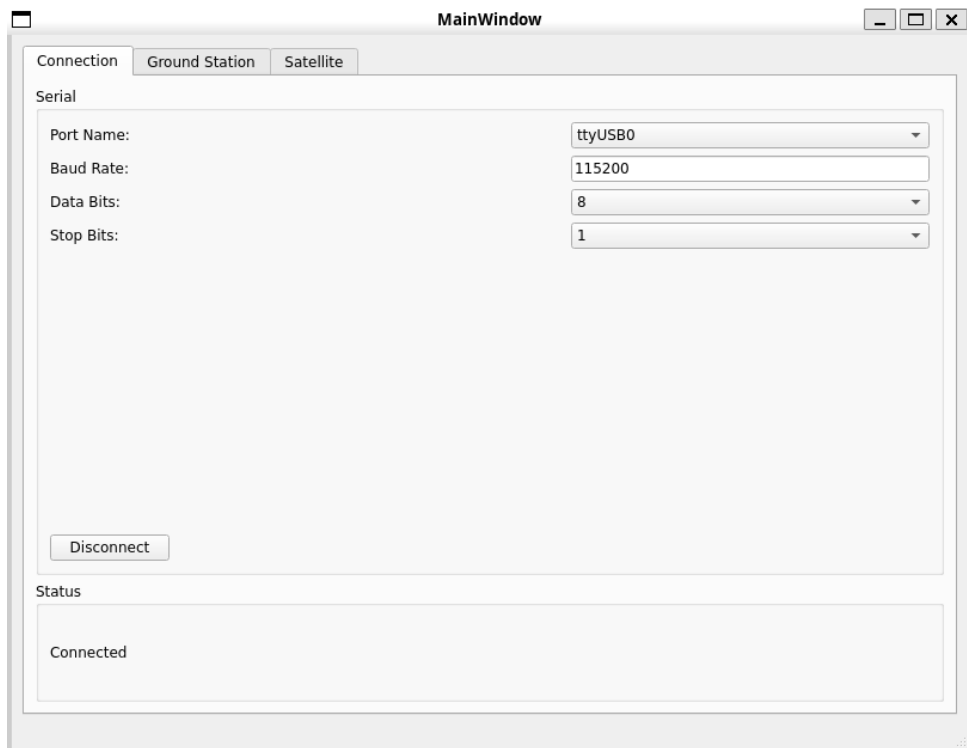


Figure F.6: GUI Output after Connecting to the Ground Station

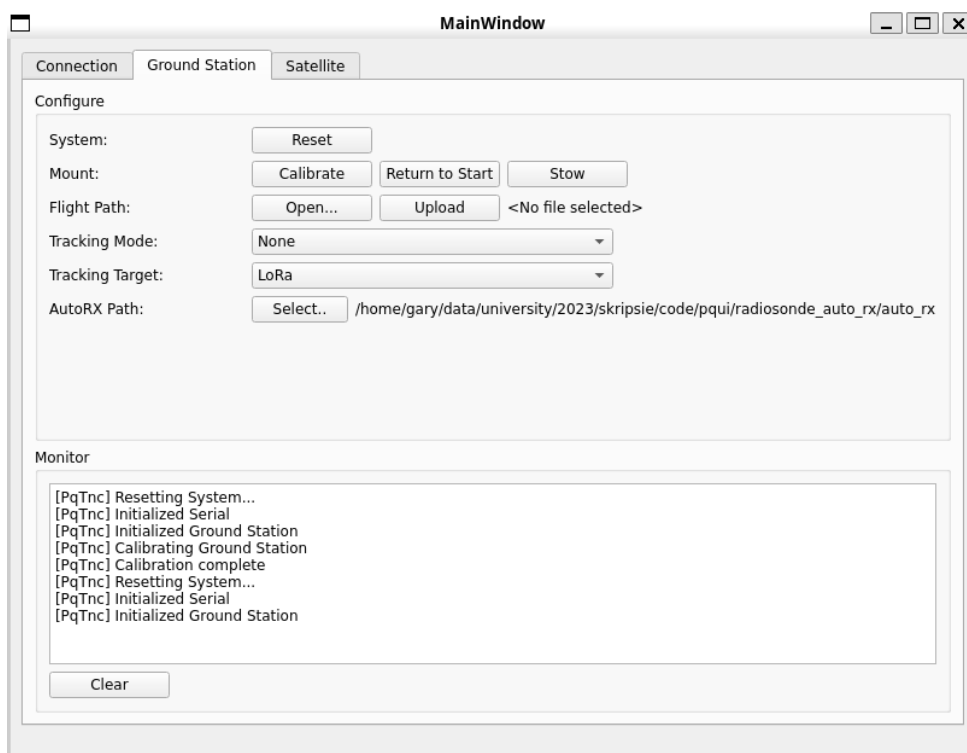


Figure F.7: GUI Output after Reset, Calibration, and Reset Again

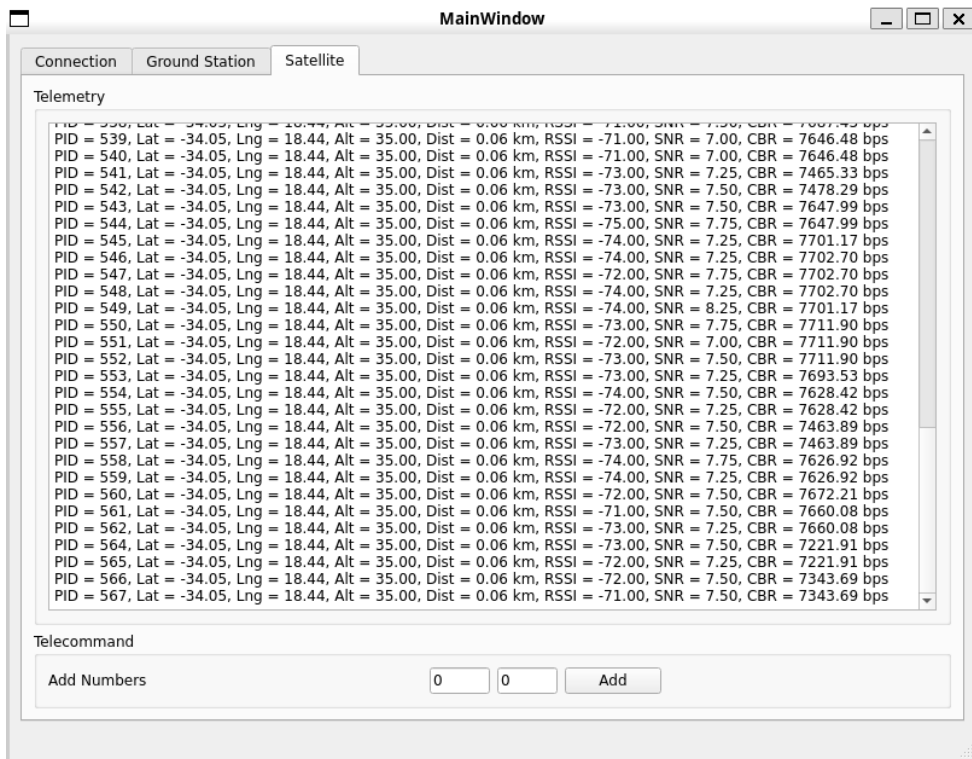


Figure F.8: GUI Output while Receiving Telemetry from LoRa Link